Erasmus University Rotterdam

Seminar Forecasting

Econometrics and Operations Research

Cost-Push vs. Demand-Pull: Evaluating the Predictive Power and Structural Dynamics of Inflation in VAR-Based Models

Team 10

Daniel Perez Domouso [1], Gabriela Cretu[2], Sitie Pan[3], Berdan Erdem [4], Orestis Tziapouras [5]

Student IDs: 616894[1], 599333[2], 656936[3], 642233[4], 619396[5]

April 14, 2025

Abstract

This paper explores how cost-push and demand-pull factors shape inflation in the Eurozone, employing multiple improved Vector Autoregressive (VAR) methodologies. Using monthly data from January 2015 to January 2024 for 14 macroeconomic indicators, our analysis contrasts traditional Structural VAR (SVAR) models with refined Bayesian SVAR (BSVAR) and Dynamic Factor-Augmented VAR (DFAVAR) approaches. This implementation better isolates and forecasts the impact of supply-side and demand-side shocks on aggregate inflation. Our work utilizes short-run recursive ordering and long-run restriction methods to overcome overparameterization and estimation uncertainty. Our results suggest that demand-side shocks tend to have a prompt and more pronounced effect on inflation in the short run, while cost-push shocks display longer-lasting effects. This result emphasizes the need for differentiated policy responses. Our results suggest that simpler, demand-focused models may improve short-term forecast accuracy; however, incorporating both supply and demand components is essential to capture sustained inflationary trends. By refining the VAR framework, the paper advances empirical methods in macroeconomic forecasting. It provides insights that could lead to more effective monetary policy in a rapidly changing global economic environment.

1 Introduction

Accurately forecasting inflation remains a significant challenge for economists and policymakers due to its dynamic and evolving nature. Inflation, commonly defined as a sustained increase in the general price level of goods and services, typically stems from two opposing forces: cost-push and demand-pull pressures. Cost-push inflation arises from increases in production costs—such as wages, raw materials, or energy—and is often triggered by supply-side shocks. Sometimes, it can lead to stagflation, where inflation rises while output remains stagnant. In contrast, demand-pull inflation occurs when aggregate demand exceeds the economy's productive capacity. This type of inflation usually emerges during periods of economic expansion, when the output gap narrows, and employment and output levels are high.

Thus, understanding and distinguishing these two inflation sources is critical, as they differ in source and persistence, and such distinction allows more accurate policy responses (Hofmann et al. (2024)). Central banks react differently depending on the source of inflation, highlighting the need to accurately understand inflation forces (Clarida et al. (1999)). Central banks tend to respond more aggressively to demand-pull inflation, often raising interest rates to reduce excess demand and contain price pressures, keeping the business cycle under control. In contrast, supply-side shocks pose a trade-off between stabilizing inflation and output, therefore requiring a more cautious approach (Clarida et al. (1999); Hofmann et al. (2024)). This difference in approach reflects the distinct nature of the two types of inflation. While demand-driven inflation calls for quick action to stabilize prices, supply-driven inflation must be carefully assessed to avoid policy decisions that could unnecessarily slow economic growth or cause persistent inflation (Bańbura et al. (2023).

Such differences in nature suggest that identification and forecasting of these two inflation components may be particularly valuable. Instead of considering inflation as one force, disentangling the influence of supply-side (cost-push) and demand-side (demand-pull) shocks on inflation can enable more targeted policymaking. This distinction is also reflected in real-world policymaking. Central banks focus on core inflation as a measure of the underlying or trend inflation, as it excludes volatile, cost-push components such as food and energy and provides a good forecast of near-term inflation (Bennett (2024) & McCracken and Ngân (2023)). However, policymakers can stabilize inflation and output more efficiently by monitoring global supply chain pressure indicators and adjusting their policy before these disruptions are passed through all inflation components (Andriantomanga et al. (2023)). Consequently, there is value in distinguishing these two components of inflation that can be addressed through monetary and fiscal tools generally demand-side pressures, and the component that arises from supply-side factors, which requires a more cautious and differentiated policy response.

In an increasingly interconnected world, understanding the drivers of inflation has become more complex and critical. Recent developments have highlighted the growing importance of both cost-push and demand-pull factors in shaping inflation dynamics. In particular, supply-side shocks such as global supply chain disruptions and energy price surges—have played a substantial role in driving inflation, especially in the aftermath of the COVID-19 pandemic and geopolitical events like the Russia-Ukraine war (Ferrante et al. (2023); Shapiro (2022); Di Giovanni et al. (2022)). These shocks have led to rising production and transportation costs, with pronounced effects observed in open economies like those in the Eurozone (Bańbura et al. (2023)), with studies confirming that such shocks lead to persistent inflationary effects Finck and Tillmann (2022); Eickmeier et al. (2023). While cost-push inflation has attracted considerable attention, demand-driven inflation remains a central concern for policymakers, particularly when formulating monetary and fiscal responses. As domestic inflation becomes increasingly sensitive to external and internal shocks, it is essential to disentangle and quantify the respective roles of demand and supply-side drivers. This study addresses this need by applying a suite of improved VAR-based models to assess how macroeconomic shocks influence aggregate inflation over different time horizons. By doing so, we aim to provide more accurate inflation forecasts and deeper insights into the transmission mechanisms of cost-push and demand-pull shocks.

Consistent with this, this paper is not only to forecast inflation accurately but also to understand how various macroeconomic shocks drive inflationary dynamics using improved VAR methodologies. A seminal foundation for inflation modeling was laid by Sims (1980), who introduced the Vector Autoregressive (VAR) model. He argued against the overuse of restrictive identification in macroeconomic

modeling and showed that VARs could capture interdependencies across variables more effectively than traditional equation-by-equation models. However, standard VARs face significant challenges when analyzing inflation dynamics: they do not distinguish between different types of structural shocks and become overparameterized when incorporating many variables and lags, which leads to poor out-of-sample forecasting performance. To overcome these limitations, researchers have extended the standard VAR to structural VAR (SVAR) models, which impose identification restrictions to separate cost-push and demand-pull shocks (Bańbura et al. (2023)). The Bayesian VAR (BVAR) framework further addresses issues of overfitting by introducing informative priors to help regularize parameter estimates in high-dimensional settings. Combining both, the Structural Bayesian VAR (SBVAR) model improves identification of structural shocks while providing greater estimation efficiency and robustness in small samples. Building on these developments, works such as Giannone et al. (2015) and Litterman (1986) highlight how Bayesian approaches enhance macroeconomic forecasting by incorporating prior beliefs and managing model uncertainty.

Our analysis utilizes monthly data spanning from January 2015 to January 2024, covering 14 macroeconomic variables that serve as robust proxies for supply-side, demand-side, and external factors influencing inflation in the Eurozone. The headline inflation rate is used as the inflation indicator, represented by the monthly growth rate of the Harmonized Index of Consumer Prices (HICP), which provides a consistent and comparable measure of overall price level changes across Eurozone countries. To assess model performance under different structural assumptions, we construct and evaluate three distinct scenarios for both the SVAR and Bayesian SVAR frameworks. Scenario 1, which serves as our baseline, includes a comprehensive set of both supply- and demand-side variables. The selection of variables for each scenario is based on theoretical relevance, statistical properties such as stationarity, and the absence of multicollinearity.

Building on this data framework, our paper extends the SVAR methodology to enhance inflation forecasting for the Eurozone. Specifically, we propose a Structural Bayesian VAR model with Minnesota priors, motivated by Chan (2021) to improve identification of cost-push and demand-pull shocks. Additionally, we employ factor-augmented methods to address high-dimensional macroeconomic data and improve shock transmission analysis(Agrippino and Ricco (2018)). By incorporating robust probabilistic forecasting techniques, we aim to provide policymakers with a clearer understanding of inflation persistence under different scenarios. While previous studies focus on general inflation forecasting, our work explicitly decomposes the aggregate inflation by capturing how various shocks propagate and persist over time. By integrating Bayesian estimation techniques, we provide a more reliable forecasting framework that offers early warning signals for persistent inflationary pressures. The central question of this study is: How can improved VAR models better forecast the effect of various shocks on inflation and analyze the persistence of these effects in the Eurozone? To answer this, we investigate the extent to which SBVAR and factor-augmented approaches improve inflation forecasting relative to traditional SVAR models. We also analyze the role of external shocks, such as global supply disruptions and commodity price surges.

By improving the accuracy of inflation forecasting, this research contributes to existing literature by proposing more effective inflation targeting for central banks and better-informed policy decisions on price stabilization measures. While this study primarily focuses on VAR based improvements, future research could explore alternative methods, such as machine learning models, for detecting nonlinear inflationary trends (Coulombe et al. (2020) and Nair and Deepa (2023)). Given the growing importance of various inflation drivers in explaining inflation dynamics, the ability to anticipate and respond to these pressures will be crucial for maintaining economic stability in the Eurozone.

The remaining paper is structured as follows. Firstly, Section 2 provides a detailed description of the data used in the analysis. Next, Section 3 outlines the methodological framework employed to identify shocks and perform inflation forecasting. Furthermore, 4 presents the empirical findings and model performance results. Finally, Section 5 concludes the paper and discusses key insights and policy implications.

2 Data

This paper includes several variables to ensure that the models used effectively capture cost-push and demand-pull dynamics and broader inflation trends. This approach aims to allow for the distinction between temporary and persistent effects of the various shocks. Further, these variables will be used to model impulse responses and forecasts. All these variables, along with their characteristics, can be found in Table 1.

Variables	Transformation	Frequency	Source
Euro area inflation rate	Growth rate	Monthly	Rate inflation
Brent Crude Oil Prices	Log-difference	Monthly	Yahoo Finance
Gas Prices	Log-difference	Monthly	FRED
Exchange rate EUR/USD	Log-difference	Every working day	ECB
Disposable income	Log-difference	Monthly	FRED
Global Economic Conditions (GECON) index	no transformation	Monthly	Baumeister et al. (2022)
Industrial production (IP)	Log-difference	Monthly	Eurostat
Gross Domestic Product (GDP)	Kalman-filtering and Log-difference	Quarterly	Eurostat
Labour Cost Index (LCI)	Kalman-filtering and Log-difference	Quarterly	Eurostat
Unemployment rate	First difference	Monthly	Eurostat
Global Supply Chain Pressure Index (GSCPI)	First difference	Monthly	NY Fed
Interest rate	First difference	Monthly	FRED
Electricity prices	Kalman-filtering and Log-difference	Quarterly	Ember
Caldara-Iacoviello Index	no transformation	Monthly	Matteo Iacoviello

Table 1: Inflation and its drivers

Note[1]*:* The paper uses Bańbura et al. (2023) as the main inspiration for the baseline specification, as their choice of variables is supported by theoretical models and empirical validation in the paper. The baseline specification consists of Brent Crude Oil Prices, Gas Prices, Euro area inflation rate, Exchange rate EUR/USD, and Disposable income. These variables are elaborated on in the subsections below. Further, most variables have been transformed to ensure stationarity and a monthly frequency for the research. Moreover, the paper uses standardization to guarantee similar scaling for all variables.

Note[2]*:* The explanations for the non-baseline variables are as follows. To begin with, the GECON index provides a broad measure of global economic activity, capturing external conditions that can influence Euro area inflation. Next, The IP provides a benchmark for how active the economy is, which helps explain movements in inflation driven by changes in domestic activity. Complementing this, the GDP reflects the overall performance of the economy beyond the industrial sector, dealing with more demand conditions, which explains a greater portion of shifts in inflation. In addition, the LCI measures total labour cost per unit of output, with rising labor costs often being passed on to consumers, contributing to inflation. Closely related, the unemployment rate helps capture the inverse relationship between inflation and labor market conditions, as suggested by the Philips Curve. To account for the influence of global supply dynamics, the paper includes the GSCPI. It measures disruptions in global production and trade networks, which directly impact the cost of goods and services and therefore inflation. Moreover, interest rates are included to capture the effects of monetary policy, which is a key driver of inflation, on inflation dynamics. Furthermore, rising electricity prices directly affect production costs for companies, and they will often pass this burden on to consumers through higher prices for goods and services. Lastly, the Caldara-Iacoviello index captures geopolitical risks such as conflicts and political instability which in turn cause external inflationary shocks.

Euro area inflation rate

As the primary variable in the research, the inflation rate reflects the overall price level changes in the Euro area, which is important in understanding the health of an economy. It is influenced by various macroeconomic factors, including the aforementioned variables in Table 1. The inflation rate plays a critical role in shaping monetary policy and helps understand the long-term effects of economic shocks in the Euro area.

Brent Crude Oil Prices

Crude oil prices, which tend to be very volatile, have a significant impact on both production costs and consumer prices. As it is used as a raw material for production but also as a fuel source, it is vital for most industries. With the cost of energy and transportation depending on the price of oil, production and distribution of the economy are impacted by it in almost all sectors. This is also confirmed by a study from Baumeister and Peersman (2013), which showed how large swings in oil prices lead to inflation by quantifying the time-varying effects of oil shocks on the US economy.

Gas Prices

Gas prices, which also tend to be volatile, directly impact budgets in households or business costs. As gas is a core fuel for transportation, the prices of goods and services can significantly increase when there are changes in gas prices, especially when it comes to frequent shipping or delivery. Closely related to Brent, Kilian and Murphy (2014) cite that fluctuations in Brent prices will cause fluctuations in gas prices. This, in turn, affects consumer spending, production costs, and inflation.

Exchange rate EUR/USD

The EUR/USD exchange rate shows how much one Euro is worth in US Dollars and is one of the most actively traded measures of currency value. Its importance lies in the fact that shifts in the rate can greatly affect trade, economic stability, and, of course, inflation. This exchange rate helps understand how external shocks are transmitted into the domestic economy. A study by Goldberg and Knetter (1997) highlights that exchange rate fluctuations are not just about currency markets; they can have real-world consequences for inflation.

Disposable income

Disposable income is the amount of money that households have left after taxes, which is then available for saving or spending. This directly measures the purchasing power of households. When disposable income rises, consumers tend to spend more, which could potentially boost economic activity and increase inflation. By tracking disposable income, the study can assess how well households change their spending in response to economic shocks. Dynan et al. (2004) show how changes in disposable income can significantly affect consumer behavior and broader economic trends, including inflation. The paper uses the DSPIC96 index, which is a US-based index. However, it uses this index as a proxy for external demand, indicating that changes in the DSPIC96 can affect European exports, production, and consequently inflation. The US economy plays a significant role in the global trade, and incorporating this index will allow the study to examine broader external pressures affecting the Euro area.

3 Methodology

Since the outbreak of the COVID-19 pandemic, the economic landscape in the Eurozone has undergone significant transformations, which fundamentally changed the dynamics of inflation. For instance, we see in the post-pandemic period that severe supply chain disruptions, shipping bottlenecks and declining manufacturing output have lead to persistent inflationary pressures. Also, geopolitical tensions, particularly the Russia-Ukraine war, have resulted in surging energy prices and rising raw material costs.

Furthermore, policy uncertainty has contributed to increased inflation volatility, making it more difficult to predict inflationary trends using conventional models such as structural VAR.

This paper first examines the theoretical framework of the Standard VAR model, which captures the dynamic relationships between macroeconomic variables without imposing prior restrictions on their interactions. While useful for analyzing correlations and forecasting, this approach does not differentiate between various types of economic shocks. To address its limitations, this paper extends its framework to incorporate identification restrictions that enable the recovery of meaningful structural shocks and facilitate an in-depth analysis of their economic impact.

We utilize a standardized VAR model incorporating both supply-side and demand-side variables:

Supply-Side Variables	**Demand-Side Variables**
Brent Crude Oil Prices (π_{Brent})	Euro area inflation rate ($\%\Delta\pi$)
Gas Prices (π_{gas})	Exchange Rate EUR/USD ($\%\Delta E_{\text{EUR/USD}}$)
Industrial Production ($\%\Delta IP$)	Unemployment rate (Δu)
Labour Cost Index ($\%\Delta LCI$)	Disposable income ($\%\Delta Y_{d,\text{US}}$)
Global Supply Chain Pressure Index ($\Delta GSCPI$)	Caldara-Iacoviello index (Γ_{CII})
Electricity prices ($\%\Delta P_{\text{elec}}$)	Gross Domestic Product ($\%\Delta GDP$)

Table 2: Supply-Side and Demand-Side Variables in the VAR Model

Note[3]*:* Interest rate ($\%\Delta i$) and Global Economic Conditions index ($GECON$) are treated as external variables, meaning that they come from outside the system that is modeled.

The subsequent sections present two distinct methodologies for model estimation: a frequentist approach, implemented using Ordinary Least Squares (OLS) with potential extensions to Instrumental Variables (IV), and a Bayesian inference approach that incorporates prior distributions to account for the inherent randomness in the structural matrix.

Despite the availability of an extensive dataset, the initial model estimation is based on a selected subset of five variables: two representing the supply side and three representing the demand side. This choice is made to address potential issues of under-identification and the limitations of OLS estimation, particularly in the context of high-dimensional systems. Our model therefore consists of the following variables:

- **Supply-side variables**: Brent Crude Oil Prices (π_{Brent}) and Gas Prices (π_{gas}).
- **Demand-side variables**: Euro area inflation rate ($\%\Delta\pi$), Exchange Rate EUR/USD ($\%\Delta E_{\text{EUR/USD}}$), and Disposable income ($\%\Delta Y_{d,\text{US}}$).

These variables form the foundation of our analysis, allowing for a systematic examination of the model's dynamics within both the frequentist and Bayesian frameworks. As the model is extended in the Bayesian context, these variables will play a crucial role in refining structural inferences.

The frequentist approach, as discussed by Kilian and Lütkepohl (2017), highlights a key challenge in models with a large number of variables—specifically, underidentification, which becomes particularly problematic when imposing long-run restrictions. This issue is extensively addressed in Chapter 11 of the referenced work. Additionally, the author underscores the difficulties of applying the Vector Error Correction Model (VECM) when the system includes more than three variables. To mitigate these challenges, we assess the stationarity and cointegration properties of the variables using economic reasoning rather than relying solely on the rank trace test, given the extensive nature of our dataset.

The paper analyzes three distinct scenarios: (1) a baseline model incorporating both supply and demand variables, (2) a model including only demand variables, and (3) an extended model that adds two external factors beyond the first scenario. Our methodological framework focuses exclusively on the first scenario, given the structural similarities among them.

3.1 Estimation of Missing Data

Given that some of the economic data used in our research is reported only on a quarterly basis, through Kalman Filter and Smoother, we estimated monthly values. Namely, the time-series for LCI and GDP are reported on a quarterly basis, hence, need estimation to be combined with monthly variables. Better techniques could be used to better estimate the missing data, yet, for the context of our study the Kalman Filter offers enough good results and allows us to extend our dataset.

The state-space representation for each variable was based on a local level trend model, where the latent monthly value is modeled as

$$x_t = x_{t-1} + w_t,$$

with w_t representing process noise, assumed to be normally distributed with initial value for the variance $\log(\sigma_x^2)$, this log transformation ensures that the variance remains positive during the optimization. The measurement equation linking the latent state to the observed quarterly data is given by

$$y_t = x_t + v_t,$$

with v_t denoting measurement error. The estimation procedure embeds quarterly observations into a monthly framework by assigning the data to every third month and estimating the process and measurement noise variances via likelihood maximization. With the parameters calibrated, the Kalman filter is applied in a recursive manner: first predicting the latent state based on previous estimates, then updating these predictions when quarterly observations are available, weighing each according to its uncertainty. A subsequent smoothing step performs a backward pass to refine the filtered estimates by incorporating future information, thereby producing a robust interpolation of monthly values that aligns with the available quarterly data.

The estimated monthly series are then combined with the rest of the monthly data framework. Diagnostic plots comparing the smoothed monthly estimates with the observed quarterly points confirm the model's performance and can be found in the appendix. This approach ensures a statistically robust interpolation of the latent monthly series from sparsely observed quarterly data.

3.2 Standard VAR Model Specification

The Standard VAR model specifies the economic variables at time t as a function of the lag variables, in addition to the contemporaneous shock:

$$Y_t = A_1 Y_{t-1} + \cdots + A_p Y_{t-p} + u_t, \text{ with } u_t \sim N(0, \Omega_{u_t}), \tag{1}$$

where Y_t is the vector of endogeneous variables and u_t is the reduced-form error term.

Following this definition, we consider

$$(Y_t)^\top = \left[(Y_t^s)^\top, (Y_t^d)^\top \right],$$

where Y_t^s represents a $m \times 1$ vector incorporating the supply-side variables, and Y_t^d represents a $(k-m) \times 1$ vector including the demand-side variables, defined as:

$$(Y_t^d)^\top = \left[\%\Delta\pi, \%\Delta Y_{d,\text{US}}, \%\Delta E_{\text{EUR/USD}} \right] \quad (Y_t^s)^\top = [\pi_{\text{Brent}}, \pi_{\text{gas}}]$$

Nonetheless, the error terms u_t may exhibit contemporaneous correlations, indicating that the shocks are not inherently structural—that is, not directly interpretable in economic terms. To identify structural shocks and to analyze the contemporaneous effects of other endogenous variables on inflation, we extend our analysis to include additional model specifications.

3.3 Structural VAR Model

The Structural VAR model extends the standard VAR model by imposing a structure on the error terms to identify structural shocks, denoted by ϵ_t. Specifically, the reduced-form errors u_t are related to the structural shocks ϵ_t through a structural impact matrix D:

$$u_t = D\epsilon_t,$$

leading to uncorrelated error terms capturing true economic interpretation (e.g., monetary policy shock, supply shock). Subsequently, after pre-multiplying the standard VAR specification by the D^{-1} structural matrix, the specification of the Structural Vector Autoregressive (SVAR) model is retrieved:

$$\begin{aligned} D^{-1}Y_t &= D^{-1}A_1Y_{t-1} + \cdots + D^{-1}A_pY_{t-p} + D^{-1}u_t \\ &= B_1Y_{t-1} + \cdots + B_pY_{t-p} + \epsilon_t, \end{aligned} \quad \text{where } B_i = D^{-1}A_i \text{ and } u_t = D\epsilon_t. \tag{2}$$

Simultaneity is a fundamental characteristic of macroeconomic models, capturing the inherent interdependence between demand-side and supply-side variables. This feature is equally relevant in the context of macroeconomic vector autoregressive (VAR) models. While the standard VAR framework provides a relatively accurate representation of the dynamic lagged relationships between variables, it is subject to identification issues. Specifically, the error terms u_t exhibit correlation, which complicates their interpretation within an economic context.

Consequently, simultaneity results in shock effects being absorbed by the error terms u_t, rather than being directly reflected in the endogenous variables. Although this formulation allows for the incorporation of indirect effects, it can obscure direct contemporaneous relationships among the endogenous variables. To establish a clear structure in the error terms, it is essential to properly identify D.

3.3.1 Identification of the Structural Matrix D

The reduced form errors u_t are linear combinations of structural shocks and thus lack direct economic interpretation. To isolate these underlying shocks, we identify the structural matrix D, which links u_t to orthogonal structural shocks ϵ_t with $E(\epsilon_t\epsilon_t') = I_k$. The reduced-form error variance-covariance matrix Ω_u, estimated via OLS, has $k(k+1)/2$ unique elements, while the structural matrix D contains k^2 parameters. Therefore, $k(k-1)/2$ additional restrictions are needed for identification. These are typically imposed using short-run and long-run restrictions.

A.Short run restrictons

Motivated by Sims (1980), we employ Cholesky decomposition on the reduced-form covariance matrix Ω_u for the short-run identification, leveraging the "world ordering" approach, where variables in the VAR model are ordered based on their response speed to different shocks. The relationship between the reduced-form covariance matrix and the structural matrix is given by:

$$\Omega_u = E\left[u_t u_t^\top\right] = DD^\top. \tag{3}$$

By applying Cholesky decomposition to Ω_u, we obtain a lower triangular matrix L such that $\Omega_u = LL^\top$. Setting $D = L$ leads to a structural matrix in the following lower triangular form:

$$D = \begin{pmatrix} d_{11} & 0 & 0 & 0 & 0 \\ d_{21} & d_{22} & 0 & 0 & 0 \\ d_{31} & d_{32} & d_{33} & 0 & 0 \\ d_{41} & d_{42} & d_{43} & d_{44} & 0 \\ d_{51} & d_{52} & d_{53} & d_{54} & d_{55} \end{pmatrix}$$

This recursive assumption imposes a natural ordering on the responses of variables to structural shocks. Specifically, the first variable responds only to its own shock, and the second variable responds to its own shock and the first shock, but not to later shocks. This structure ensures that some shocks do not immediately affect certain variables, aligning with economic intuition.

The ordering of variables in the model is instrumental in delineating the causal relationships among them, governing which variables exert contemporaneous effects and which have lagged impacts. Our approach prioritizes supply-side factors first, as their impact is immediate—for example, increases in oil or gas prices result in an instantaneous response in inflation Asab (2025). Conversely, demand-side variables—specifically foreign disposable income and exchange rates—are positioned later. These external factors do not operate in the short run; rather, their effects materialize only after a delay, once the channels transmitting the shocks(e.g. trade and exports) have fully absorbed the initial impacts Obstfeld and Rogoff (2000). Once the structural matrix D is identified, the structural shocks can be recovered as:

$$\varepsilon_t = D^{-1} u_t.$$

Sign restrictions

While zero-restrictions are effective for identification in the short-run, we cannot disregard the dynamic and continuous interaction between variables, as dictated by economic theory. Specifically, there may be a consistently positive or negative short-run causal effect. To capture this, we used an approach to identify D in a SVAR model by imposing sign restrictions on the impulse responses through an iterative guess-and-check method, as proposed by Kilian and Murphy (2012).

The intuition behind this method is grounded in theoretical reasoning, where some economic shocks are expected to cause only increases or decreases in one or more of the endogenous variables. For instance, an oil supply shock is expected to drive core inflation upwards. These expected directional responses form the basis for the sign restrictions, as outlined in the table below, which shows the expected signs for shocks affecting the endogenous variables in Y_t:

The guess-and-check method is employed to find the appropriate rotation of the structural matrix D that aligns with the expected positive or effects.

To begin the identification process, we start with an initial guess for D by setting it as the Cholesky decomposition of the reduced-form covariance matrix, as discussed in the context of short-run restrictions. However, since the matrix D is not uniquely identified, we explore different potential rotations of D by multiplying it by a random orthgonal matrix Q to generate different rotations, where $QQ' = I_k$:

$$D^* = DQ,$$

here, matrix D^* represents the rotated structural matrix D.

After applying the rotation, we compute the Impulse Response Functions (IRFs) corresponding to the structural shocks implied by the rotated matrix D^*. If the computed IRFs align with the imposed sign restrictions, the random rotation matrix Q is accepted, and the corresponding D^* remains valid, otherwise we generate a new rotation matrix. This process is repeated iteratively until a matrix D^* is found that satisfies all the imposed sign restrictions. By iteratively testing different rotations of the structural matrix D, the guess-and-check method allows us to identify a matrix that ensures the shocks' impacts on the endogenous variables are consistent with the theoretical expectations.

Based on the previously defined short-run restrictions, the contemporaneous effects among the variables are identified as follows. Additionally, these restrictions are imposed as penalties when computing the D matrix.

Variable \ Shocks	Oil	Gas	Inflationary	Expansionary US income	Euro Appreciation
π_{Brent}	+	0	0	0	0
π_{gas}	*	+	0	0	0
$\%\Delta\pi$	+	+	+	0	0
$\%\Delta Y_{d,\text{US}}$	*	*	*	+	0
$\%\Delta E_{\text{EUR/USD}}$	*	*	-	*	+

Table 3: Impact of Various Shocks on Different Variables

B.Long-run restrictons

Building on the work of Blanchard and Quah (1988), who first applied long-run restrictions to output and the unemployment rate using a VAR framework, we propose extending this approach to analyze cost-push and demand-pull shocks. Specifically, we impose long-run restrictions on all variables from both the supply and demand sides within the benchmark model to capture their persistence. This extension is motivated by the well-established understanding that demand-side shocks typically have a short-lived impact, whereas supply-side shocks have a more persistent and widespread effect on inflation.

In the original paper, the focus is on the output gap and unemployment. In contrast, our analysis incorporates all variables in the first scenario, after addressing issues of cointegration and stationarity.

Starting from the standard vector autoregressive process of order p from section 3.2

$$Y_t = A_1 Y_{t-1} + A_2 Y_{t-2} + \cdots + A_p Y_{t-p} + u_t, \tag{4}$$

where Y_t is a $k \times 1$ vector of endogenous variables, A_i are $n \times n$ coefficient matrices, and u_t is a $k \times 1$ vector of white noise error terms with mean zero and covariance matrix Σ_u.

Using the lag operator L, defined as $L^j Y_t = Y_{t-j}$, we rewrite the equation compactly as:

$$A(L)Y_t = u_t, \tag{5}$$

where the lag polynomial is given by:

$$A(L) = I - A_1 L - A_2 L^2 - \cdots - A_p L^p. \tag{6}$$

If the process is stable, meaning that the determinant $\det(A(L)) = 0$ has all its roots outside the unit circle, then $A(L)$ is invertible and can be expressed as an infinite power series:

$$A(L)^{-1} = \sum_{j=0}^{\infty} C_j L^j. \tag{7}$$

Consequently, multiplying both sides of equation 5 by $A(L)^{-1}$, we obtain the moving average representation:

$$Y_t = \sum_{j=0}^{\infty} C_j u_{t-j}. \tag{8}$$

This expresses Y_t as an infinite sum of past shocks(see Appendix A), where the matrices C_j capture the dynamic response of the system to innovations. This representation is useful for studying impulse responses and forecasting in time series analysis.

The shocks captured in this reduced-form VAR can be divided into shocks on the supply side and shocks on the demand side, which can be defined as a $m \times 1$ vector v_t^s and a $(k-m) \times 1$ vector v_t^d, respectively:

$$u_t = D \begin{pmatrix} \epsilon_t^s \\ \epsilon_t^d \end{pmatrix}; \quad \begin{pmatrix} Y_t^s \\ Y_t^d \end{pmatrix} = \sum_{j=0}^{\infty} \tilde{C}_j \begin{pmatrix} \epsilon_{t-j}^s \\ \epsilon_{t-j}^d \end{pmatrix}, \tag{9}$$

where $\tilde{C}_j = C_j D$. Identification relies on the assumption that only supply shocks have a lasting impact on supply-side factors, such as gas and oil prices. In contrast, demand shocks—originating from foreign disposable income and exchange rate fluctuations—are assumed to exert only transitory effects on these supply-side variables. Assume for simplicity that:

$$\tilde{C}_j = \begin{bmatrix} \tilde{c}_j^{(s)} \\ \tilde{c}_j^{(d)} \end{bmatrix}, \tag{10}$$

where $\tilde{c}_j^{(s)}$ is the coefficient associated with the structural shocks on the **supply** side, and $\tilde{c}_j^{(d)}$ is the coefficient associated with the structural shocks on the **demand** side, in the moving average representation

at time j. Consider the impulse response of a variable in Y_t, in our case $\%\Delta\pi$, to the structural shocks represented by

$$\begin{bmatrix} \epsilon^s_{t-j} \\ \epsilon^d_{t-j} \end{bmatrix}.$$

We know that

$$\pi_t = \pi_{t-1} + \%\Delta\pi_t = \pi_{t-j} + \sum_{i=0}^{j-1} \%\Delta\pi_{t-i},$$

so:

$$\frac{\partial\, \pi_t}{\partial \begin{bmatrix} \epsilon^s_{t-j} \\ \epsilon^d_{t-j} \end{bmatrix}} = \sum_{i=1}^{j} \tilde{c}^{(d)}_{i,p} \tag{11}$$

$$\rightarrow \sum_{i=1}^{\infty} \tilde{c}^{(d)}_{i,p} \tag{12}$$

where p is the index of inflation in the demand side vector of coefficients.

We consider the following identification matrix:

$$\sum_{i=1}^{\infty} \tilde{c}_i = \begin{pmatrix} j_{11} & j_{12} & j_{13} & 0 & 0 \\ j_{21} & j_{22} & j_{23} & 0 & 0 \\ j_{31} & j_{32} & j_{33} & j_{34} & j_{35} \\ j_{41} & j_{42} & j_{43} & j_{44} & j_{45} \\ j_{51} & j_{52} & j_{53} & j_{54} & j_{55} \end{pmatrix}, \tag{13}$$

based on the assumption that demand-side variables do not affect supply-side dynamics in the long run. Given our focus on disentangling cost-push and demand-pull drivers of inflation, we allow both types of shocks to exert persistent effects on inflation in the long-run.

We know that based on equation 7, the following holds true:

$$\sum_{i=1}^{\infty} \tilde{C}_j = \left(\sum_{i=1}^{\infty} C_j\right) D = C(1)D = A(1)^{-1}D, \quad \text{where } C(L) = \sum_j C_j L^j = A(L)^{-1},$$

.

$$\begin{bmatrix} \%\Delta\pi_t \\ \%\Delta Y_{d,\mathrm{US},t} \\ \%\Delta E_{\mathrm{EUR/USD},t} \\ \pi_{\mathrm{Brent},t} \\ \%\Delta\pi_{\mathrm{gas},t} \end{bmatrix} = (I_k - A(L)) \begin{bmatrix} \%\Delta\pi_{t-1} \\ \%\Delta Y_{d,\mathrm{US},t-1} \\ \%\Delta E_{\mathrm{EUR/USD},t-1} \\ \pi_{\mathrm{Brent},t-1} \\ \%\Delta\pi_{\mathrm{gas},t-1} \end{bmatrix} + u_t \tag{14}$$

is the VAR regression, where k is the number of variables i.e. 5 in our scenario. We consider the next steps to identify the impact of the structural shocks incorporating the long-run restrictins, i.e. the D matrix.

Step 1 Run OLS regression $Y_t = A_1 Y_{t-1} + \ldots + A_p Y_{t-p} + e_t$, get OLS coefficients $A_1, \ldots, A_p$ and variance of the residuals Ω

Step 2 Find D such that

$$\left(I_k - \sum_{j=1}^{p} A_j\right)^{-1} D = \begin{pmatrix} * & * & * & 0 & 0 \\ * & * & * & 0 & 0 \\ * & * & * & * & * \\ * & * & * & * & * \\ * & * & * & * & * \end{pmatrix} \quad \text{and} \quad \Omega = DD^\top.$$

3.4 Bayesian Vector Autoregressions

The Structural VAR (SVAR) model serves as a fundamental framework for capturing the dynamic relationships between macroeconomic variables, as developed in papers Wang and McPhail (2014) and Dungey and Pagan (2000). However, SVAR models estimated using frequentist methods such as Maximum Likelihood Estimation (MLE) or Generalized Method of Moments (GMM) face several limitations, particularly in high-dimensional settings where overfitting and estimation uncertainty become prominent issues. Additionally, frequentist methods treat parameters as fixed but unknown, relying on large sampling variability and asymptotic properties for inference.

Unlike frequentist approaches, Bayesian methods as developed in (Giannone et al. (2015) and Chan (2021)) treat parameters as random variables with probability distributions, enabling quantification of parameter uncertainty. By introducing a Structural Bayesian VAR (SBVAR), the priors are imposed for addressing the limitations of SVAR, particularly in handling structural breaks, preventing overfitting, and enabling probabilistic forecasts.

3.4.1 Recursive Structural Bayesian Vector Autoregressions

The recursive Structural Bayesian Vector Autoregression (SBVAR) method aligns with our frequentist approach in the specification of the D matrix. However, it offers enhanced flexibility and is better suited for handling high-dimensional datasets. To capture the recursive relationships between variables in the D matrix, we employ the LKJ distrubution introduced by Lewandowski et al. (2009).

The LKJ distribution is used to identify positive-definite covariance matrices, characterized by a shape parameter η. A covariance matrix Σ is obtained via the decomposition:

$$\Sigma = \mathbf{DRD}^T \tag{15}$$

where $\mathbf{D}$ is a lower triangular matrix (in our case, the structural matrix from Cholesky decomposition) and $\mathbf{R}$ is a diagonal matrix, often the identity matrix. The shape parameter η controls the concentration of the distribution around the identity matrix, ensuring valid correlation structures.

The distribution first generates a seed to obtain the correlation matrix $\mathbf{R}$. The probability density function for a $k \times k$ matrix $\mathbf{R}$ is:

$$p(\mathbf{R}; \eta) = C \times [\det(\mathbf{R})]^{\eta-1}$$

where C is the normalizing constant, given by:

$$C = 2^{\sum_{k=1}^{d-1}(2\eta-2+d-k)(d-k)} \prod_{k=1}^{d-1} \left[B\left(\eta + \frac{d-k-1}{2}, \eta + \frac{d-k-1}{2}\right)\right]^{d-k}$$

When $\eta = 1$, the distribution is uniform over the space of all correlation matrices, meaning it is uniform over the set of positive definite matrices with a unit diagonal.

The previously discussed restrictions remain valid under the Bayesian recursive approach, being implemented as tensor constraints during the matrix generation process. The priors on the coefficients are specified in the same manner as in the non-recursive structural Bayesian VAR framework, with further details provided in the next subsection.3.4.2

3.4.2 Non-recursive Structural Bayesian Vector Autoregressions

The SBVAR model follows the structural VAR representation but incorporates Bayesian priors, shown as follows:

$$\begin{aligned} D^{-1}Y_t &= D^{-1}A_1Y_{t-1} + \cdots + D^{-1}A_pY_{t-p} + \epsilon_t \\ &= B_1Y_{t-1} + \cdots + B_pY_{t-p} + \epsilon_t, \end{aligned} \quad \text{where } B_i = D^{-1}A_i \text{ and } u_t = D\epsilon_t. \tag{16}$$

To estimate the system, this paper introduces three main components: (1) prior distributions for coefficients B_i, scaling matrix D^{-1} and covariance matrix Σ_ϵ, (2) posterior inference, and (3) MCMC sampling.

Minnesota priors on coefficients B_i

Following the studies conducted by Giannone et al. (2015) and Chan (2021), this paper imposes the most commonly used prior in Bayesian analysis, Minnesota prior, to regularize the coefficients, which is essential for improving estimation efficiency and preventing overfitting in high-dimensional settings. The Minnesota prior assumes that each coefficient follows a normal distribution:

$$B_i \sim \mathcal{N}(0, V_{i,kk}),$$

where $V_{i,kk}$ is a diagonal variance matrix, which determines the degree of shrinkage applied to the coefficients. The variance structure is specified as follows, drawing from Chan (2021):

$$V_{i,kk} = \begin{cases} \frac{\lambda_1}{l^2}, & \text{for the coefficient on the } l\text{-th lag of variable } i \text{ (own lag)} \\ \frac{\lambda_2 s_i^2}{l^2 s_j^2}, & \text{for the coefficient on the } l\text{-th lag of variable } j, j \neq i \text{ (cross-lag)} \end{cases}$$

where λ_1, λ_2 and λ_3 are shrinkage parameters controlling prior belief strength. Additionally, s_i^2 and s_j^2 are the sample variances of residuals of variables i and j, respectively, estimated using a standard VAR model. This variance structure ensures that the coefficients for higher lags are shrunk more heavily, preventing overfitting of distant lags that may not have meaningful economic relationships. The introduction of Bayesian priors allows for a model that can adjust to changing relationships over time, especially when there are significant shifts in the economic environment.

The term $\frac{1}{l^2}$ of the variance matrix $V_{i,kk}$ ensures that the coefficients in the higher lags shrink more, reducing the risk of overfitting the distant lag relationships. For own lags, the shrinkage becomes stronger as the lag order increases:

$$V_{i,kk} \propto \frac{1}{l^2}.$$

Shrinkage works by pulling the parameter estimates toward the prior mean, which results in a penalty for large coefficients unless the data strongly suggests they are important. For cross-lagged terms, the shrinkage depends on the relative variability of the variables. If s_i^2 is much larger than s_j^2, the model will shrink the cross-lagged coefficients more, reflecting that the relationship between the variables may not be as strong. For the intercept, the shrinkage depends on the variability of the variable itself, ensuring that intercepts for more variable series receive less shrinkage.

Priors for scaling matrix D^{-1} and variance-covariance matrix Σ_ϵ

In addition to priors for coefficients, the paper also introduces priors for D^{-1} and Σ_ϵ. The former represents a scaling of the endogenous variables, constrained by identification strategy, and the latter is the variance-covariance matrix of the structural errors.

A common choice for these priors is the Inverse-Wishart distribution (Agrippino and Ricco (2018)). This distribution is commonly used for covariance matrices in Bayesian models because it is a conjugate prior. As we consider a structural var, we consider this prior applied to our The priors can be written as:

$$D^{-1} \sim IW(\Psi_0, \nu_0) \text{ and } \Sigma_\epsilon \sim IW(\Psi_0, \nu_0).$$

Ψ_0 represents the scale matrix, which corresponds to the prior beliefs about the scale and structure of the covariance matrix and ν_0 is the degrees of freedom parameter that determine how informative the prior is. For instance, a large ν_0 gives a more diffuse prior, while a small ν_0 implies stronger belief in the scale matrix Ψ_0. The choice of Ψ_0 and ν_0 depend on prior beliefs about the structure of D^{-1} and Σ_ϵ. When little prior knowledge is available, the weakly informative prior is chosen to ensure that our model remains flexible and that the data primarily drives the estimation process. Particularly, the paper assumes each variable has a unit variance and that there is no prior preference for any particular correlation structure by setting Ψ_0 equal to identity matrix. Similarly, setting ν_0 = k+1 ensures that the prior is minimally informative while still being a valid Inverse-Wishart distribution, with k the dimension of the matrix.

Identification in SVAR models revolves around the estimation of D^{-1} through external economic restrictions. In the Bayesian approach, rather than estimating the coefficients directly, we impose prior probability distributions.

Posterior distribution

In a Bayesian context, the posterior distribution of the parameters in the SVAR model can be derived using Bayes' theorem, which combines the likelihood of the data with the prior beliefs about the coefficients, error covariance, and scaling matrix. The parameters need to be estimated are coefficient matrices Bi, scaling matrix D^{-1} and covariance matrix of structural shocks Σ_ϵ. The paper assumes that the errors ϵ_t are normally distributed with mean 0 and covariance matrix Σ_ϵ. The likelihood of function of the data is written as:

$$L(\theta \mid Y) = \prod_{t=1}^{T} N(Y_t \mid X_t\beta, \Sigma_\epsilon) = \prod_{t=1}^{T} \frac{1}{(2\pi)^{k/2}|\Sigma_\epsilon|^{1/2}} \exp\left(-\frac{1}{2}\epsilon_t^T \Sigma_\epsilon^{-1} \epsilon_t\right),$$

where X_t is the matrix of lagged variables $Y_{t-1}, Y_{t-2}, ..., Y_{t-p}$, $\beta = [B_1, B_2, ..., B_p]$ is the coefficient matrix of the model, and θ represents the set of all model parameters $(B_1, B_2, ..., B_p, D^{-1}, \Sigma_\epsilon)$. The dimension of Y_t is k.

Based on the Bayes' Theorem, the posterior distribution of the parameters given the data is proportional to the product of probability of observing the data given the parameters and the prior beliefs about B_i, D^{-1} and Σ_ϵ (Giannone et al. (2015)):

$$p(\theta \mid Y) \propto \prod_{t=1}^{T} N(Y_t \mid X_t\beta, \Sigma_\epsilon) \cdot \prod_{i=1}^{p} N(B_i \mid 0, \Sigma_B) \cdot IW(D^{-1} \mid \Psi_0, \nu_0) \cdot IW(\Sigma_\epsilon \mid \Psi_0, \nu_0).$$

In a Bayesian analysis, the parameters are estimated by drawing samples from this posterior distribution using Markov Chain Monte Carlo methods.

Markov Chain Monte Carlo (MCMC) sampling

Since the posterior distribution cannot generally be computed analytically due to the complex structure of the model, the paper uses Markov Chain Monte Carlo (MCMC) methods, specifically Gibbs sampling, to generate samples from the posterior distribution. The central idea of MCMC process is to draw a sequence of samples from the joint posterior distribution of the parameters $\theta = (B_1, B_2, \ldots, B_p, D^{-1}, \Sigma_\epsilon)$, generating a Markov chain that eventually converges to the target posterior distribution.

Motivated by Agrippino and Ricco (2018), Gibbs sampling involves iteratively sampling from the conditional distributions of each parameter, given the current values of the others. More specifically, the paper samples from the conditional distribution for B_i given D^{-1} and Σ_ϵ, for D^{-1} given B_i and Σ_ϵ, and for Σ_ϵ given B_i and D^{-1}. The posterior distribution of B_i given D^{-1} and Σ_ϵ is as follows:

$$p(B_i \mid Y, D^{-1}, \Sigma_\epsilon) \propto N(B_i \mid 0, \Sigma_B) \prod_{t=1}^{T} N(Y_t \mid X_t B_i, \Sigma_\epsilon).$$

$$\begin{aligned} B_i \mid Y, D^{-1}, \Sigma_\epsilon &\sim \mathcal{N}(M_B, V_B), \\ \text{where } V_B &= (X^\top X + \Sigma_B^{-1})^{-1}, \\ M_B &= V_B X^\top Y. \end{aligned}$$

The conditional distribution of D^{-1} given B_i and Σ_ϵ is an Inverse-Wishart distribution:

$$p(D^{-1} \mid Y, B_i, \Sigma_\epsilon) \propto \mathcal{IW}(D^{-1} \mid \Psi_0, \nu_0)$$

with posterior-updated parameters Ψ_0' and ν_0', computed conditional on B_i, Σ_ϵ, and the observed data:

$$\Psi_0' = \Psi_0 + \sum_{t=1}^{T}(Y_t - X_t B_i)(Y_t - X_t B_i)^\top,$$
$$\nu_0' = \nu_0 + T.$$

Therefore, the paper samples from:

$$D^{-1} \mid Y, B_i, \Sigma_\epsilon \sim \mathcal{IW}(\Psi_0', \nu_0')$$

Similarly, the conditional posterior distribution of Σ_ϵ follows an Inverse-Wishart distribution as well, where samples originate from:

$$\Sigma_\epsilon \mid Y, B_i, D^{-1} \sim \mathcal{IW}(\Psi_0', \nu_0')$$

After a sufficient number of iterations, the MCMC process converges to the true posterior distribution with a vector of N posterior samples $\theta^{(1)}, \theta^{(2)}, \ldots, \theta^{(N)}$, which can be used to estimate the posterior means of the parameters and compute confidence intervals from the posterior samples:

$$\hat{\theta} = \frac{1}{N}\sum_{k=1}^{N}\theta^{(k)}$$

$$CI_\theta = (\theta_{(2.5\%)}, \theta_{(97.5\%)})$$

Interpretation of Shocks on Inflation

Once the structural shocks are identified, the paper examines their short-term impact on inflation using Impulse Response Functions (IRF), defined as follows:

$$\text{IRF}_{\pi,s}(h) = \frac{\partial \pi_{t+h}}{\partial s_t}$$

where π_{t+h} represents the inflation after h periods of shocks. Using the IRFs allows us to analyze how inflation reacts to different economic shocks in the short term and identify which shocks have the most persistent effects. Additionally, varying the forecast horizon helps determine whether inflation adjusts gradually over time or experiences an immediate response to a given shock.

While Structural Bayesian VAR (SBVAR) improves upon the standard SVAR model by incorporating Bayesian priors to prevent overfitting, it still faces challenges related to multicollinearity among variables. To address this limitation, the paper extends the SBVAR framework to a Dynamic Factor Model (DFM) in the following subsection.

3.5 Factor augmented vector auroegressions

In practice, all the previously mentioned Structural Vector Autoregression (SVAR) methods break down when a key assumption fails—specifically, the assumption that the structural matrix D is invertible. This reliance can result in misleading outcomes that fail to accurately capture the true behavior of inflation. The problem becomes especially pronounced when dealing with a large number of endogenous variables, which often introduces multicollinearity.

Subsequently, time series models frequently suffer from the "curse of dimensionality" in such cases, leading to overparameterization and estimation inefficiencies. To address this, prior research has proposed the use of factor-augmented models, which condense the common variation across many time series into a smaller set of latent factors. This approach reduces the model's dimensionality while retaining essential macroeconomic dynamics. A prominent example is the Factor-Augmented VAR (FAVAR) model developed by Bernanke et al. (2005).

Dynamic Factor Model Specification

The dynamic factor model assumes that the observed variables, denoted as Y_t, can be decomposed into a small number of dynamic factors f_t and an idiosyncratic component v_{it}. Specifically, let Y_t be an $k \times 1$ stationary vector observed over $t = 1, \ldots, T$. Assume both k and T are large. The latent factors f_t, a $q \times 1$ vector, capture the common sources of variation in the observed variables.In our scenario, we set $q = 2$ to distinguish between the two types of shocks, assigning supply-side variables to one factor and demand-side variables to the other.

The model assumes that each component $y_{i,t}$ of Y_t follows the factor structure

$$y_{i,t} = \tilde{\lambda}_i(L) f_t + v_{i,t}, \tag{17}$$

where $\tilde{\lambda}_i(L)$ is a lag polynomial of order p. The idiosyncratic component $v_{i,t}$ may exhibit serial correlation, modeled as

$$v_{i,t} = \delta_i(L) u_{i,t-1} + w_{i,t}, \tag{18}$$

where $\delta_i(L)$ is a lag polynomial (i.e., a finite-order lag operator) and $w_{i,t}$ is a white noise process.

The dynamic factors f_t follow a vector autoregressive (VAR) process, modeled as

$$f_t = \Gamma(L) f_{t-1} + \eta_t, \tag{19}$$

where $\Gamma(L)$ is a lag polynomial, and η_t represents a vector of factor innovations.

Assumptions

To ensure the proper identification of the factor model, the following assumptions are imposed:

- $E[v_{i,t} v_{j,s}] = 0$ for all $i \neq j$, implying that all common variation is captured by the factors.
- $E[f_t v_{i,s}] = 0$, ensuring that factors and idiosyncratic components are uncorrelated.
- $E[w_{i,s} w_{i,t}] = 0$ for all $s \neq t$, meaning that the idiosyncratic errors are not serially correlated.

This setup is known as an exact dynamic factor model, in which all covariance among variables is fully explained by the factors. It is exact because of the first assumption, and is dynamic because both current and lagged factors affect y_{it}.

Transformation into a VAR Representation

To derive a reduced-form representation, equation 18 must be substituted into equation 17:

$$(I - \delta_i(L)L) y_{i,t} = \lambda_i(L) f_t + w_{i,t} \quad \text{where } \lambda_i(L) = (I - \delta_i(L)L)\tilde{\lambda}_i(L).$$

This equation provides an alternative specification of the model. The system can also be written in matrix form, where $D(L)$ is a block diagonal matrix capturing the dynamics of the idiosyncratic components.

$$Y_t = D(L) Y_{t-1} + \lambda_i(L) f_t + w_t \quad \text{where } D(L) = \begin{bmatrix} \delta_1(L) & \ldots & 0 \\ \vdots & \ddots & \vdots \\ 0 & \ldots & \delta_n(L). \end{bmatrix}.$$

The model can also be rewritten in static form by introducing an augmented factor vector:

$$\begin{aligned} Y_t &= D(L) Y_{t-1} + \Lambda F_t + w_t \\ F_t &= \Phi(L) F_{t-1} + G \eta_t, \end{aligned} \quad \text{where } F_t = [f_{t-1}, \ldots, f_{t-p}].$$

Finally, we can write everything together as a VAR:

$$\begin{bmatrix} F_t \\ Y_t \end{bmatrix} = \begin{bmatrix} \Phi(L) & 0 \\ \Lambda\Phi(L) & D(L) \end{bmatrix} \begin{bmatrix} F_{t-1} \\ Y_{t-1} \end{bmatrix} + \begin{bmatrix} I & 0 \\ \Lambda & I \end{bmatrix} \varepsilon_t, \quad \varepsilon_t = G\eta_t + w_t. \tag{20}$$

3.6 Forecast Evaluation

This research examines various forecast evaluation methods that measure both prediction accuracy and robustness in order to evaluate the forecasting performance of the models. Specifically, model performance is evaluated using Root Mean Squared Error (RMSE):

$$\text{RMSE} = \sqrt{\frac{1}{n}\sum_{i=1}^{n}(y_i - \hat{y}_i)^2}$$

4 Results

As described in the previous section, we performed numerical experiments on the models using Python 3.12.4 on an Apple M1 2020 with 8 GB of RAM. The objective is to explore how macroeconomic shocks, both from the demand-side and supply-side, affect inflation across different time horizons using improved VAR models: SVAR, Bayesian SVAR (BSVAR), and Dynamic Factor-Augmented VAR (DFAVAR). This section begins by introducing three model scenarios, where we select variables based on their theoretical relevance, stationarity, and lack of multicollinearity. For the SVAR model, we first examine how shocks to one variable influence others within the system, considering both short- and long-term effects. We then present the Impulse Response Functions (IRFs) for inflation in response to various shocks across all three scenarios. Following this, we present the point estimates and distributions of the parameters obtained using the Bayesian approach and compare the corresponding IRFs with the SVAR model. Additionally, we introduce a fourth scenario that incorporates more supply-side variables to enable a comparison between the BSVAR and DFAVAR models. Finally, we evaluate the out-of-sample forecasting accuracy of each model using the Root Mean Squared Error (RMSE). Based on this analysis, we aim to determine which model provides the best predictions of inflation and offers insights into how inflation dynamics are driven by demand-pull and cost-push factors.

4.1 Variables Selection

The selection of variables for the three scenarios is based on their theoretical relevance, stationarity properties, and lack of multicollinearity. Each variable is chosen for its economic significance in explaining inflation dynamics. We conducted the Augmented Dickey-Fuller (ADF) stationarity test over our estimation period from January 2015 to December 2022 on all variables in the dataset, and some were found to be non-stationary, even after log-differencing or other transformations. As stationarity is a critical assumption for VAR-based models, these non-stationary variables were excluded from the analysis.

The correlation matrix of the remaining variables is shown in Figure 1, where we select those that are not highly correlated with each other to avoid multicollinearity and cointegration issues. In Scenario 1, we include variables from both demand and supply sides, as shown below:

$$\left(Y_t^{\text{Scenario 1}}\right)^\top = \left[\pi_{\text{Brent}},\, \pi_{\text{gas}},\, \%\Delta\pi,\, \%\Delta Y_{d,US},\, \%\Delta E_{\text{EUR/USD}}\right]$$

Here, all the selected variables are stationary. The π_{Brent} and π_{gas} are included as key supply-side indicators as these are commonly identified in the literature as primary drivers of cost-push inflation. To capture demand-side dynamics, $\%\Delta Y_{d,US}$ and $\%\Delta E_{\text{EUR/USD}}$ are incorporated to reflect changes in consumer spending and exchange rate movements, respectively. Scenario 2 isolates the impact of demand-side shocks by excluding the supply-side variables present in Scenario 1:

$$\left(Y_t^{\text{Scenario 2}}\right)^\top = \left[\%\Delta\pi,\, \%\Delta Y_{d,US},\, \%\Delta E_{\text{EUR/USD}}\right]$$

Scenario 3 expands on Scenario 1 by incorporating the $GECON$ index and interest rate $\%\Delta i$ to account for the role of global economic activity and central bank policy in shaping inflationary pressures, shown as follows:

$$\left(Y_t^{\text{Scenario 3}}\right)^\top = [\pi_{\text{Brent}},\, \pi_{\text{gas}},\, \%\Delta\pi,\, GECON,\, \%\Delta i,\, \%\Delta Y_{d,US},\, \%\Delta E_{\text{EUR-USD}}]$$

During the stationarity tests over our estimation period, we found that variables such as GDP, unemployment rate, and GSCPI were non-stationary, even after transformation. These variables were therefore excluded from the models. As seen in Figure 1, several variables remain for potential inclusion, which will be considered in the fourth scenario, where we compare the BSVAR model with the DFAVAR model.

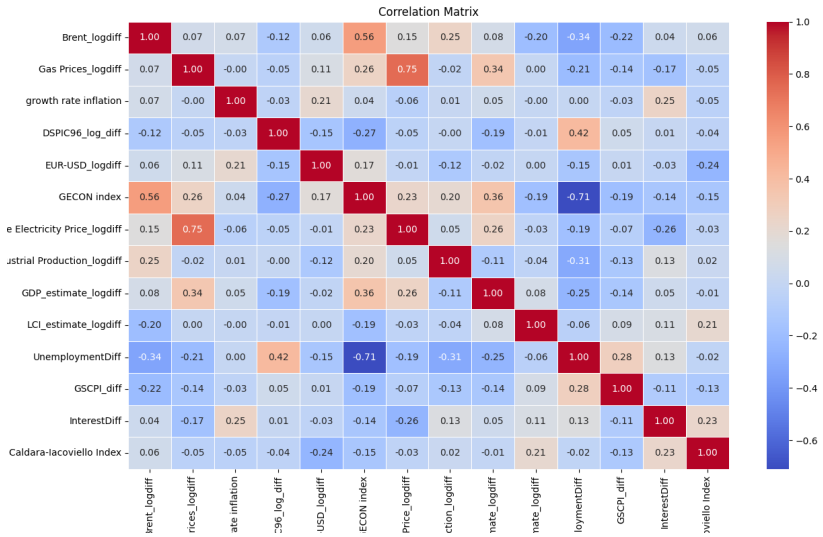

Figure 1: Correlation Matrix of all variables

4.2 Structural Vector Autoregressive Model

For each scenario, we determine the optimal lag length by estimating the normal Vector Autoregressions (VARs) and comparing the Akaike Information Criterion (AIC), Hannan-Quinn Criterion (HQ), and Bayesian Information Criterion (BIC). These information criteria help balance model fit with parsimony by penalizing models with excessive parameters that could lead to overfitting and this is especially important in the context of our relatively short sample period and limited number of variables.

In our case, the Akaike Information Criterion (AIC) suggests an optimal lag length of 7, the Hannan-Quinn Criterion (HQ) recommends a lag of 2, and the Bayesian Information Criterion (BIC) points to a lag length of 1. Given our relatively small sample size and the risk of overfitting with higher-order models, we adopt the BIC's recommendation of a single lag which imposes a stronger penalty for model complexity compared to AIC and HQ and is thus more suitable for small datasets where parsimony is crucial. This conservative approach is particularly important in our context for analyzing SVAR and BSVAR approaches, as we aim to maintain robustness across multiple model specifications.

4.2.1 Structural Identification

To estimate the structural model presented in Equation 3.3, we impose a set of identification restrictions as outlined in the methodology section. These restrictions allow us to recover the structural matrix D from the reduced-form representation. This matrix not only captures the transformation between these two types of shocks but also reflects the contemporaneous interactions among variables. By applying

a recursive identification scheme in each scenario, we assume that a structural shock can only contemporaneously influence the variables ordered after its corresponding variable in the system. We focus on presenting the structural matrix and long-run impact matrix for Scenario 1 in the main text as this scenario represents a balanced specification that includes both demand-side and supply-side variables and thus offers a comprehensive view of the inflation dynamics. Models 2 and 3, while still relevant, are either more restricted or more extended. Including the detailed identification matrices for each model in the main text would risk redundancy, thus we provide the corresponding matrices for Models 2 and 3 in the Appendix.

Table 4 presents the estimated structural D matrix for Scenario 1 which captures the contemporaneous relationships between structural shocks and reduced-form innovations. The identification strategy relies on sign restrictions and a recursive structure imposed via Cholesky decomposition, resulting in a lower triangular matrix. In this framework, the ordering of variables determines the assumed contemporaneous causal structure: structural shocks to variables listed earlier in the ordering can contemporaneously affect those that follow, but not vice versa. Since Brent oil prices are placed first in the ordering, their shocks can contemporaneously influence all other variables in the system. In contrast, shocks to the EUR/USD exchange rate are contemporaneously influenced by all preceding shocks.

Notably, the diagonal elements of this matrix are close to 1, which indicates that each structural shock is largely explained by its own reduced-form shocks. Further, the coefficient of 0.0006 on the Brent oil price shock in the gas price equation suggests a very small negative contemporaneous effect. This finding is consistent with the low empirical correlation (0.07) observed between Brent oil and gas prices in Figure 1. Additionaly, when considering the contemporaneous impact of both cost-push factors on CPI inflation, we observe small positive effects: 0.0426 for Brent and 0.0001 for gas, which explains the theoretical expectation of cost-push inflation, where increases in input prices contribute to upward pressure on consumer prices.

Table 4: Structural D Matrix for Scenario 1

	π_{Brent}	π_{gas}	$\%\Delta\pi$	$\%\Delta Y_{d,US}$	$\%\Delta E_{\text{EUR-USD}}$
π_{Brent}	0.9175	0.0000	0.0000	0.0000	0.0000
π_{gas}	-0.0006	0.9517	0.0000	0.0000	0.0000
$\%\Delta\pi$	0.0426	-0.0001	0.9912	0.0000	0.0000
$\%\Delta Y_{d,US}$	-0.0600	-0.0889	-0.0358	0.7956	0.0000
$\%\Delta E_{\text{EUR-USD}}$	0.0533	0.1093	0.2017	-0.2191	0.8761

4.2.2 Long-Run Impact Analysis

While the structural matrix shown in Table 4 captures the contemporaneous effects of structural shocks, Table 5, denoted as $C_j D$ in the methodology section, reflects the cumulative effects of each structural shock on all variables in the system. These long-run impacts can be interpreted in two ways: the diagonal elements that are close to or greater than 1 indicate that a variable's own shock has a persistent long-term effect, while the off-diagonal elements represent spillover effects, capturing how a shock to one variable influences others in the system over time. Given our focus on analyzing the long-term effects of various macroeconomic shocks on inflation dynamics, particular attention is paid to the third row of the matrix, which corresponds to the long-run drivers of inflation. The results suggest that cost-push shocks, particularly those from Brent oil prices and gas prices, have moderate but persistent effects on inflation over the long run. Notably, while the Brent shock has a positive influence (0.1589), the effect of gas prices is slightly negative (-0.1435). Conversely, demand-side shocks—represented by disposable income ($\%\Delta Y_{d,US}$) and the exchange rate exhibit ignorable long-run influence on inflation, as their corresponding entries in the third row are close to zero.

Table 5: Long-Run Impact Matrix $C(\infty) \cdot D$ for Scenario 1

	π_{Brent}	π_{gas}	$\%\Delta\pi$	$\%\Delta Y_{d,US}$	$\%\Delta E_{\text{EUR-USD}}$
π_{Brent}	1.3577	-0.1100	-0.0705	0.0085	0.2348
π_{gas}	0.3514	1.0848	-0.0090	-0.0905	0.2401
$\%\Delta\pi$	0.1589	-0.1435	0.9239	0.0133	-0.0607
$\%\Delta Y_{d,US}$	-0.2138	-0.1055	-0.0022	0.4948	0.0053
$\%\Delta E_{\text{EUR-USD}}$	-0.0862	-0.1622	0.2970	-0.2728	1.1999

Below Figure 2 presents the impulse responses of the growth rate of inflation to shocks originating from Brent oil prices, gas prices, disposable income, and the exchange rate in Scenario 1. The results indicate that supply-side shocks (from Brent and gas prices) exert moderate but persistent effects on inflation over time, with their impacts lingering for a longer duration. In contrast, demand-side shocks (from disposable income and the exchange rate) cause a significant initial spike in inflation growth, but their effects drop down quickly after around 70 periods. The speed of convergence to zero is notably faster for demand-side shocks, whereas supply-side shocks maintain a more sustained influence on inflation. Ultimately, the effects of all shocks on inflation growth fade away completely.

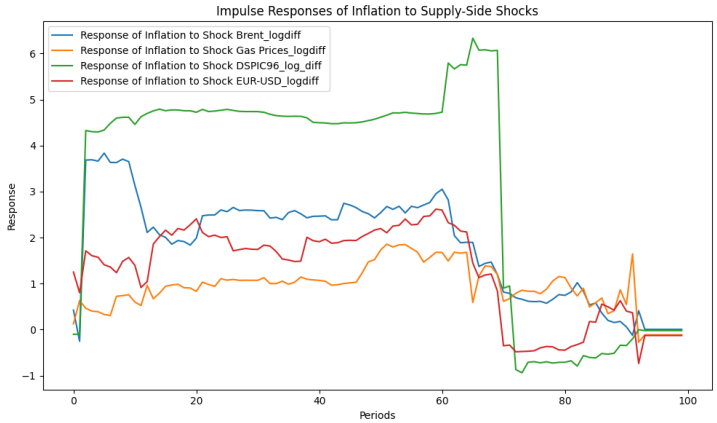

Figure 2: Impulse responses of Scenario 1

Similar patterns emerge in Figure 3 and 4, which visualize the impulse responses of inflation to shocks in Scenario 2 and Scenario 3. As in Scenario 1, supply-side shocks (such as those from Brent oil and gas prices) exhibit a persistent influence on inflation over time. However, demand-side shocks (including those from disposable income and the exchange rate) show a more temporary effect by causing an immediate spike in inflation that gradually fades. Looking specifically to the left panel plot for Scenario 3, an important observation is the substantial and persistent effect of shocks stemming from global economic conditions $GECON$ in both scenarios. These shocks capture broader external factors such as global economic growth, international trade disruptions, a d commodity price shifts, and thus appear to have a dominant and long-lasting effect on inflation in the Eurozone. The impulse responses show that the effects of these global shocks reach their maximum magnitude after approximately sixty months and remain significant even after 100 months. Notably, this effect surpasses that of any domestic supply or demand shocks, which suggests that global economic conditions play a crucial role in determining inflation dynamics.

Unlike the previous scenarios, we also notice that not all shocks in Scenario 3 converge to zero, even after a long period of 100 months. Specifically, the interest rate shock, representing monetary policy actions, exhibits a slightly negative effect on inflation in the long run. This suggests that tight monetary policies may have a delayed but persistent dampening effect on inflation, with the influence lingering even after a long horizon. The negative effect of interest rate shocks is consistent with the general theory that higher interest rates reduce inflationary pressures over time by cooling consumption and investment. This

pattern suggests that while global economic shocks dominate in the short to medium term, monetary policy actions can also have lasting effects on inflation in the long run, though less immediate. These findings underscore the role of domestic monetary policy measures and external factors in shaping inflation outcomes in the Eurozone.

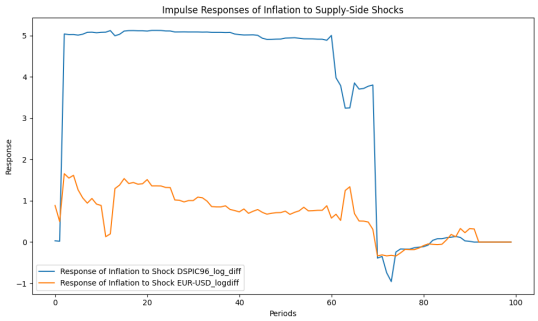

Figure 3: Impulse responses of Scenario 2

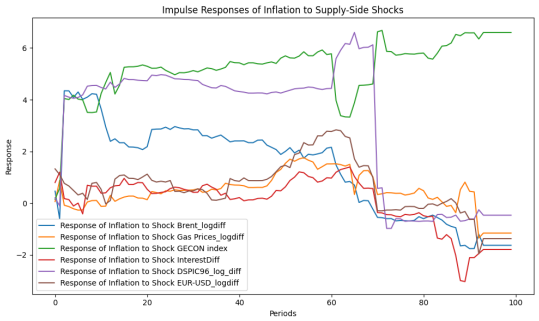

Figure 4: Impulse responses of Scenario 3

4.2.3 SVAR-based Inflation Forecasts and Accuracy Evaluation

To evaluate the forecasting performance of the SVAR model, we forecast the growth rate of inflation for each of the scenarios. Figure 5 below compares the forecasted growth rate of inflation from each scenario with the actual observed values over a 12-month horizon from January 2023 to January 2024.

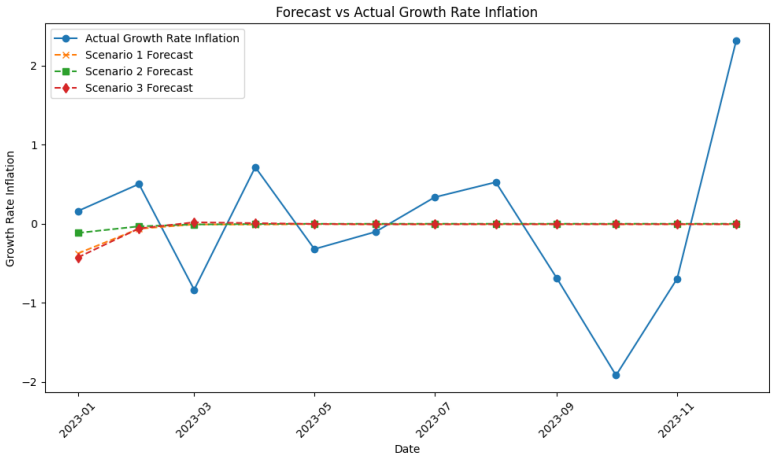

Figure 5: Growth rate inflation forecast of all models vs actual growth rate inflation

From the figure, we observe that the differences in forecast performance across scenarios are relatively small. However, Scenario 2 (demand-only variables) shows slightly better accuracy in the short-term horizons, particularly at the beginning of the forecast period. This suggests that demand-side variables may carry more predictive power for short-term inflation dynamics, which is consistent with findings discusses earlier. Further, using a broader set of variables, as in Scenario 3, does not necessarily lead to better forecasting performance especially in the short run. This implies that parsimony yields better forecasts over shorter horizons when performing forecasts using SVAR mmodel. It's also important to note that a model using only supply-side variables was not feasible in our study. This is in line with much of the literature, which emphasizes that demand-side factors play a dominant role in forecasting inflation in the short term while supply shocks often have more persistent but delayed effects and are generally not sufficient on their own for effective inflation forecasting.

The forecasting accuracy of the SVAR model across each scenario is evaluated using the Root Mean Squared Error (RMSE), as shown in Table 6 and visualized in Figure 6. The results clearly indicate that Scenario 2 achieves the lowest RMSE at the 1-month horizon (0.2765), compared to 0.5360 in Scenario 1 and 0.5862 in Scenario 3. This superior performance of Scenario 2 persists across the short-term horizons. For example, at the 2-month horizon, Scenario 2 maintains a lower RMSE (0.4261) than both Scenario 1 (0.5510) and Scenario 3 (0.5744). However, as the forecast horizon extends to the medium and long term, the discrepancies across scenarios diminish. At the 12-month horizon, RMSE values converge to 1.0031 for Scenario 2, 1.0135 for Scenario 1, and 1.0165 for Scenario 3. We also observe that while the more parsimonious and demand-driven specification in Scenario 2 enhances short-term forecasting accuracy, it lacks the capacity to fully capture the broader inflation dynamics that unfold over the longer term, which indicates the limitations of conventional SVAR models when forecasting inflation over extended horizons thus this is where our Bayesian approach comes in.

Table 6: Forecast RMSE for Scenarios 1–3

Horizons	**Scenario 1**	**Scenario 2**	**Scenario 3**
1	0.5360	0.2765	0.5862
2	0.5510	0.4261	0.5744
3	0.6556	0.5898	0.6799
4	0.6740	0.6247	0.6871
5	0.6192	0.5767	0.6308
6	0.5666	0.5281	0.5771
7	0.5401	0.5051	0.5497
8	0.5390	0.5078	0.5475
9	0.5571	0.5310	0.5643
10	0.8028	0.7881	0.8073
11	0.7931	0.7800	0.7973
12	1.0135	1.0031	1.0165

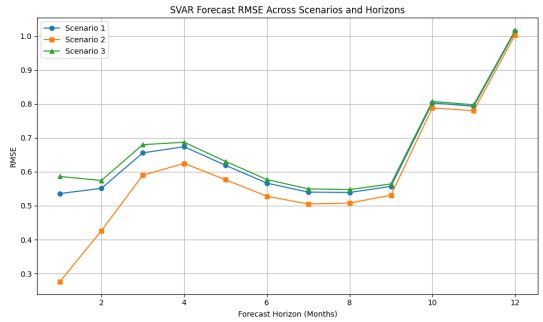

Figure 6: RMSE of SVAR inflation forecasts across scenarios

4.3 Bayesian Structural Autoregressive Model (BSVAR)

4.3.1 Identification of Structural Matrix: Recursive and Non-Recursive Approaches

As described in the methodology section, the relationship between structural shocks in the BSVAR model is captured by imposing prior distributions on the coefficients matrix and then sampling from the posterior distribution using a Monte Carlo Markov Chain (MCMC) algorithm. This process generates a distribution of coefficient estimates. For clarity and interpretability, we take the mean of these estimates only for Scenario 1. The results for the structural matrix D are presented in Tables 7 and 8, representing the non-recursive and recursive Bayesian approaches, respectively.

Table 7: Point Estimates for structural matrix D (mean of posterior) — Scenario 1, non-recursive BSVAR

	π_{Brent}	π_{gas}	$\%\Delta\pi$	$\%\Delta Y_{d,US}$	$\%\Delta E_{\text{EUR-USD}}$
π_{Brent}	-0.4030	0.1269	-0.4079	0.1246	-0.0081
π_{gas}	0.1647	-0.3292	-0.3466	0.1580	0.0197
$\%\Delta\pi$	0.5193	0.4989	0.1691	0.4767	0.3880
$\%\Delta Y_{d,US}$	0.1078	0.0920	-0.4714	-0.5296	-0.0524
$\%\Delta E_{\text{EUR-USD}}$	-0.2655	-0.2299	-0.1516	-0.4435	0.2739

Table 8: Point Estimates for Structural Matrix D (mean of posterior) — Scenario 1, recursive BSVAR

	π_{Brent}	π_{gas}	$\%\Delta\pi$	$\%\Delta Y_{d,US}$	$\%\Delta E_{\text{EUR-USD}}$
π_{Brent}	1.0299	0.0000	0.0000	0.0000	0.0000
π_{gas}	0.0228	1.0050	0.0000	0.0000	0.0000
$\%\Delta\pi$	0.0727	0.0828	0.9690	0.0000	0.0000
$\%\Delta Y_{d,US}$	0.0712	0.0994	0.0421	1.2063	0.0000
$\%\Delta E_{\text{EUR-USD}}$	-0.0319	-0.0937	-0.1985	0.2762	1.0905

From these tables, we observe that in the non-recursive approach, the matrix D is fully parameterized in order to allow for contemporaneous interaction among all variables. In contrast, the recursive specification imposes a lower triangular structure on D which reflects a recursive identification strategy where each variable is contemporaneously affected only by those ordered before it. Analyzing the results, we find that the growth rate of inflation is largely driven by its own shocks (0.9690) in the recursive model. Further, the effect of cost-push factors appears to be relatively small, which aligns with our earlier findings using the SVAR model in Table 4. However, in the non-recursive setup, inflation is significantly affected by Brendt oil and gas prices (0.5193 and 0.4989) and also shows notable contemporaneous feedback from disposable income from the USA (0.4767) and the exchange rate (0.3880). This suggests that the non-recursive estimation captures a more complex and multi-directional relationship, which potentially offers a more flexible depiction of interdependencies among the variables.

While the SVAR framework requires a recursive ordering to identify structural shocks, the non-recursive BSVAR allows for more flexible identification without such restrictions. Though allowing for richer contemporaneous relationships goes at the cost of increased estimation complexity and the potential risk of overfitting. In the following subsections, we compare the impulse response functions derived from both BSVAR approaches across the three scenarios to assess whether recursive ordering improves the interpretability and robustness of the results.

4.3.2 Comparison of Impulse Responses Across Scenarios

Figure 7 and 8 compare the impulse responses of the growth rate of inflation to various structural shocks using the non-recursive and recursive Bayesian Structural VAR (BSVAR) approaches under Scenario 1. A clear difference from the standard SVAR model emerges: in this BSVAR framework, both supply and demand shocks generate moderate but immediate responses in inflation, which decay rapidly within just a few periods. This is in contrast to the SVAR model discussed earlier, where the effects of such supply shocks often linger and diminish slowly, sometimes persisting up to 70 periods. This difference can be explained by the regularization properties of the Bayesian approach. In BSVAR, prior distributions are imposed on the parameters, which helps constrain implausible dynamics and reduces the persistence of shocks that may arise due to overfitting or multicollinearity in standard SVAR models. As a result, the BSVAR model produces sharper, more realistic responses that reflect the inherent uncertainty and variability in macroeconomic relationships.

Moreover, while demand-side shocks, such as those from disposable income and exchange rate fluctuations, have traditionally been considered to have strong immediate in their effects on inflation, the BSVAR model reveals moderate short-term impacts. This may stem from the way Bayesian estimation combines observed data with economic theory, allowing even demand shocks to have less influence when supported by the data.

The non-recursive BSVAR shown in Figure 7, uses a fully parameterized structural matrix which enables contemporaneous interactions among all variables. This flexibility captures a complex, multi-directional system in which inflation is simultaneously influenced by shocks to commodity prices, income, and exchange rates. On the other hand, the recursive BSVAR shown in Figure 8 enforces a lower-triangular structure on the matrix of contemporaneous relationships. Here, inflation can only respond contemporaneously to variables that precede it in the assumed ordering. While this identification strategy is easier to interpret and grounded in traditional macroeconomic theory, it might underestimate the actual influence of contemporaneous shocks due to its structural rigidity.

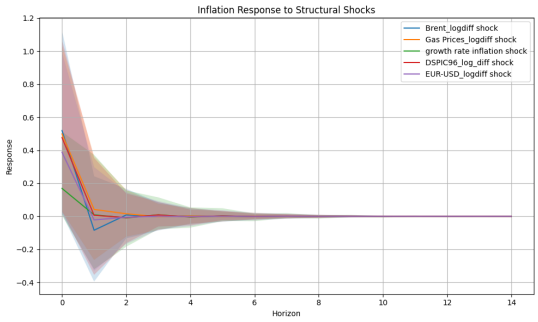

Figure 7: Impulse responses of Scenario 1 using non-recursive ordering

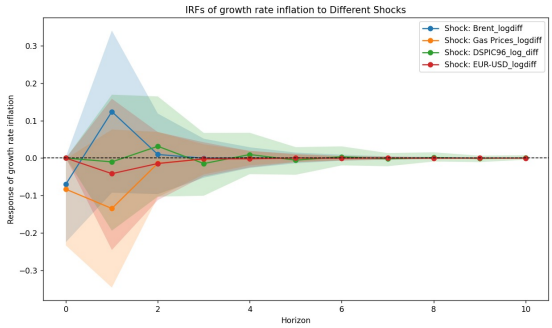

Figure 8: Impulse responses of Scenario 1 using recursive ordering

4.3.3 BSVAR-based Inflation Forecasts and Accuracy Evaluation

Table 9 presents the Root Mean Squared Error (RMSE) across 12 forecast horizons for both the non-recursive and recursive BSVAR approaches with each evaluated under three distinct scenarios. A key observation from here is that the recursive and non-recursive BSVAR models yield nearly identical forecast accuracy across all horizons. This similarity is expected, as both models are built upon the same reduced-form VAR which is estimated using Bayesian methods. The forecasting process in VAR models relies primarily on the reduced-form coefficients, instead of the structural identification scheme used to recover structural shocks. Since we imposed identical prior distributions in estimating both versions of the BSVAR model, comparing the forecast accuracy between the recursive and non-recursive BSVAR approaches is not informative.

Table 9: RMSE Values — Non-Recursive vs. Recursive BSVAR, Across Scenarios

Horizon	**Non-Recursive**			**Recursive**		
	Scenario 1	Scenario 2	Scenario 3	Scenario 1	Scenario 2	Scenario 3
1	0.512531	0.287056	0.582537	0.5286	0.2786	0.5818
2	0.532874	0.430972	0.570338	0.5446	0.4258	0.5687
3	0.648941	0.592143	0.679967	0.6525	0.5898	0.6773
4	0.667362	0.626260	0.685899	0.6706	0.6246	0.6844
5	0.613999	0.578117	0.630222	0.6168	0.5766	0.6290
6	0.562024	0.529381	0.576787	0.5645	0.5280	0.5756
7	0.535477	0.506209	0.548874	0.5377	0.5050	0.5479
8	0.534284	0.508680	0.546065	0.5363	0.5076	0.5452
9	0.553759	0.531873	0.563853	0.5555	0.5310	0.5631
10	0.802062	0.788636	0.808382	0.8031	0.7881	0.8079
11	0.792925	0.780583	0.798736	0.7939	0.7801	0.7982
12	1.012247	1.003410	1.016420	1.0129	1.0031	1.0161

A more meaningful comparison can be drawn between the SVAR and BSVAR models. As shown in Table 6 and 9, both models exhibit comparable forecast performance across all horizons. While the BSVAR framework offers several theoretical advantages, such as regularization, improved robustness in small samples, and the integration of prior beliefs as outlined in the methodology section, it does not demonstrate superior predictive power relative to the SVAR approach in our case. This suggests that the SVAR model was already well-specified and estimated on a reasonable dataset, which indicates the additional structure and shrinkage imposed by the Bayesian approach are less meaningful in terms of forecasting accuracy.

Nonetheless, the value of the BSVAR approach extends beyond forecast performance as it also enhances the structural interpretation of inflation dynamics. By incorporating informative priors on the coefficients, BSVAR facilitates a more transparent analysis of how inflation responds to various structural shocks. As demonstrated earlier, this framework enables us to empirically evaluate and challenge theo-

retical assumptions. While conventional economic theory assumes that demand-side shocks exert strong short-run effects on inflation, which is supported by SVAR estimations shown earlier. The reliability of such conclusions may be questionable in our settings with limited data. In addition, SVAR relies on frequentist estimation, which can be unstable and biased in small samples. In contrast, BSVAR ensures more plausible and stable parameter estimates by leveraging Bayesian priors on coefficients to regularize the estimation process. Moreover, the Bayesian framework allows for the estimation of full posterior distributions of model parameters, rather than relying solely on point estimates. This feature enables us to construct confidence intervals for impulse responses, shown in 7 and 8.

Therefore, by comparing both recursive and non-recursive structures, we observe that the BSVAR model reveals slightly different patterns of contemporaneous relationships. This comparative approach offers a more comprehensive view of macroeconomic interactions and illustrates the trade-offs between structural assumptions and empirical flexibility.

4.4 Dynamic Factor Model Augmentation

5 Conclusion

Appendix

A Theorem and Proof of the Moving Average Representation

Given a stable VAR(p) process of the form:

$$Y_t = A_1 Y_{t-1} + A_2 Y_{t-2} + \cdots + A_p Y_{t-p} + e_t, \tag{21}$$

if the roots of the characteristic polynomial $\det(A(L)) = 0$ *lie outside the unit circle, then the process can be written as a moving average (MA) process of infinite order:*

$$Y_t = \sum_{j=0}^{\infty} C_j e_{t-j}. \tag{22}$$

Proof Sketch. The VAR(p) process can be expressed in lag operator form as:

$$A(L)Y_t = e_t, \tag{23}$$

where $A(L) = I - A_1 L - A_2 L^2 - \cdots - A_p L^p$ is the lag polynomial. Under the stability condition that the roots of the characteristic equation $\det(A(L)) = 0$ lie outside the unit circle, the lag polynomial $A(L)$ is invertible. By the Neumann series (see Appendix B), we can write the inverse of $A(L)$ as:

$$A(L)^{-1} = \sum_{j=0}^{\infty} C_j L^j, \tag{24}$$

where the series converges, and therefore:

$$Y_t = A(L)^{-1} e_t = \sum_{j=0}^{\infty} C_j e_{t-j}. \tag{25}$$

B Neumann Series and Invertibility of Lag Polynomials

Theorem (Neumann Series). Suppose that T is a bounded linear operator on a normed vector space X. If the Neumann series converges in the operator norm, then $I - T$ is invertible and its inverse is given by:

$$(I - T)^{-1} = \sum_{k=0}^{\infty} T^k, \tag{26}$$

where I is the identity operator in X.

Proof Sketch. Consider the partial sums:

$$S_n := \sum_{k=0}^{n} T^k. \tag{27}$$

Then:

$$\begin{aligned}
(I - T)S_n &= (I - T)\sum_{k=0}^{n} T^k && (28)\\
&= \sum_{k=0}^{n} T^k - \sum_{k=0}^{n} T^{k+1} && (29)\\
&= I - T^{n+1}. && (30)
\end{aligned}$$

Taking the limit as $n \to \infty$ and assuming that $\|T\| < 1$, we obtain:

$$\lim_{n\to\infty} (I - T)S_n = I. \tag{31}$$

Thus, $(I - T)$ is invertible and:

$$(I - T)^{-1} = \sum_{k=0}^{\infty} T^k. \tag{32}$$

This result is analogous to the geometric series in R. In the context of the VAR(p) process, T corresponds to the lag polynomial operator $A(L)$, and the invertibility condition corresponds to the stability of the process (all eigenvalues outside the unit circle).

C Optimized structural matrix and long-run impact matrix of Model 2 and 3

Table 10: Structural D Matrix for Model 2

	$\%\Delta\pi$	$\%\Delta Y_{d,US}$	$\%\Delta E_{\text{EUR-USD}}$
$\%\Delta\pi$	1.0075	0.0000	0.0000
$\%\Delta Y_{d,US}$	-0.0469	0.8277	0.0000
$\%\Delta E_{\text{EUR-USD}}$	0.2226	-0.1929	0.9128

Table 11: Long-Run Impact Matrix $C(\infty) \cdot D$ for Model 2

	$\%\Delta\pi$	$\%\Delta Y_{d,US}$	$\%\Delta E_{\text{EUR-USD}}$
$\%\Delta\pi$	0.9534	-0.0042	-0.0681
$\%\Delta Y_{d,US}$	-0.0261	0.5226	0.0342
$\%\Delta E_{\text{EUR-USD}}$	0.3157	-0.2450	1.2987

Table 12: Structural D Matrix for Model 3

	π_{Brent}	π_{gas}	$\%\Delta\pi$	$GECON$	$\%\Delta i$	$\%\Delta Y_{d,US}$	$\%\Delta E_{\text{EUR-USD}}$
π_{Brent}	0.8994	0.0000	0.0000	0.0000	0.0000	0.0000	0.0000
π_{gas}	-0.0000	0.9348	0.0000	0.0000	0.0000	0.0000	0.0000
$\%\Delta\pi$	0.0705	-0.0000	0.9842	0.0000	0.0000	0.0000	0.0000
$GECON$	0.4608	0.0733	-0.0713	0.5673	0.0000	0.0000	0.0000
$\%\Delta i$	0.0005	-0.1856	0.3073	-0.0003	0.8751	0.0000	0.0000
$\%\Delta Y_{d,US}$	-0.1092	-0.0316	-0.0195	-0.0000	-0.0372	0.7136	0.0000
$\%\Delta E_{\text{EUR-USD}}$	0.1069	0.0636	0.1778	0.1228	0.0464	-0.1566	0.8121

Table 13: Long-Run Impact Matrix $C(\infty) \cdot D$ for Model 3

	π_{Brent}	π_{gas}	$\%\Delta\pi$	$GECON$	$\%\Delta i$	$\%\Delta Y_{d,US}$	$\%\Delta E_{\text{EUR-USD}}$
π_{Brent}	1.2201	-0.0828	-0.0245	-0.1262	0.1219	-0.0261	0.2313
π_{gas}	0.4806	1.0128	-0.0744	0.1986	-0.1283	-0.0230	0.2076
$\%\Delta\pi$	0.1583	-0.1418	0.9153	-0.0334	-0.0290	0.0043	-0.0554
$GECON$	1.3723	0.0797	-0.1631	0.7789	-0.1002	0.0826	0.2103
$\%\Delta i$	0.0829	0.0312	0.5298	-0.0653	1.1479	-0.0322	-0.1037
$\%\Delta Y_{d,US}$	-0.3902	-0.0558	0.0349	-0.1924	-0.0146	0.3962	0.0177
$\%\Delta E_{\text{EUR-USD}}$	0.0784	-0.3120	0.1341	0.3138	-0.3640	-0.1340	1.0901

D IRFs of Model 1-3 with supply and demand separated

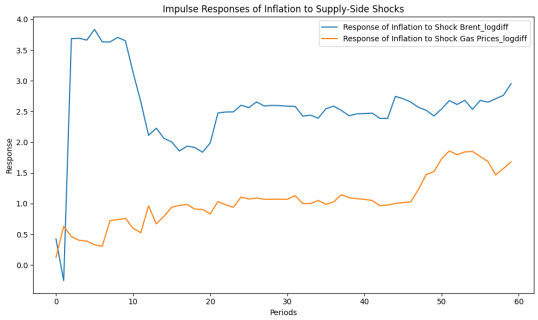

Figure 9: Impulse responses to supply shocks of Model 1

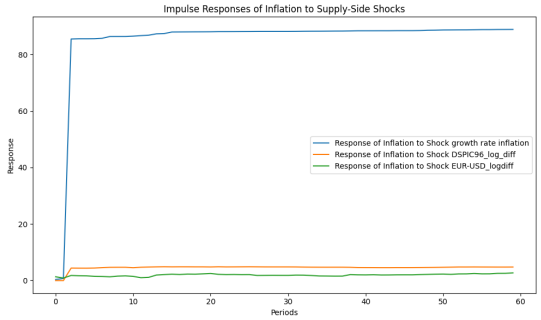

Figure 10: Impulse responses to demand shocks of Model 1

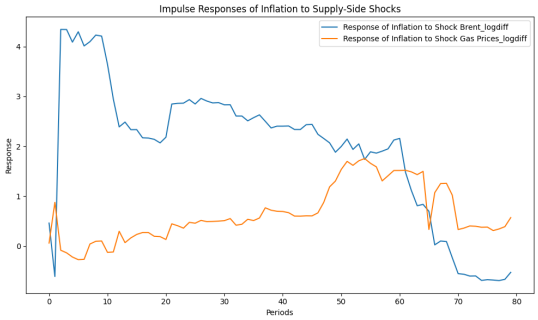

Figure 11: Impulse responses to supply shocks of Model 3

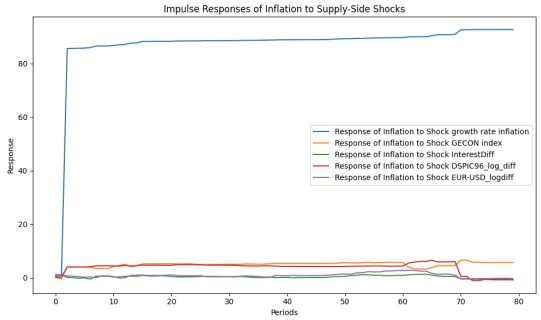

Figure 12: Impulse responses to demand shocks of Model 3

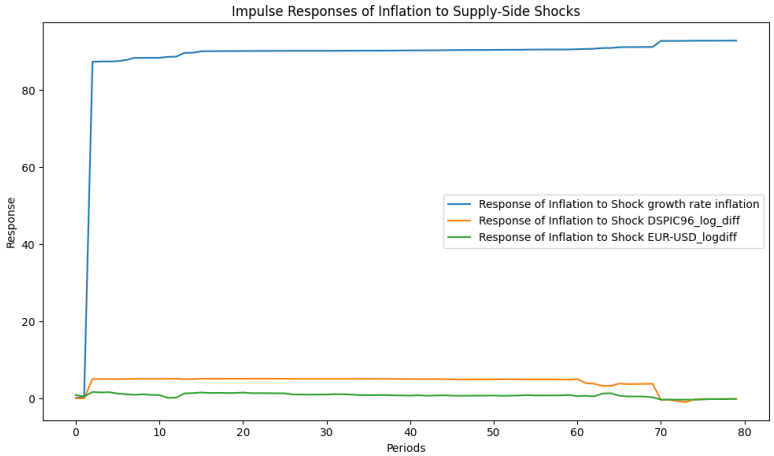

Figure 13: Impulse responses to demand shocks of Model 2

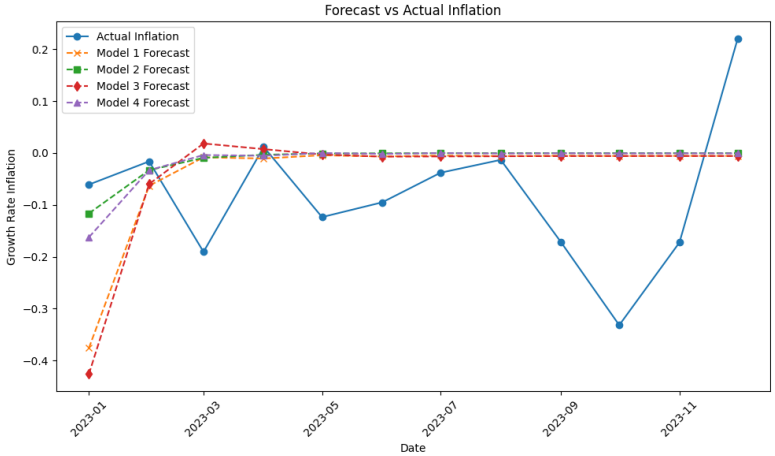

Figure 14: Growth rate inflation forecast of all models vs actual growth rate inflation

E Bayesian B matrices Model 2-3

Table 14: Point Estimates of Coefficient Matrix B (Model 1)

	π_{Brent}	π_{gas}	$\%\Delta\pi$	$\%\Delta Y_{d,US}$	$\%\Delta E_{\text{EUR-USD}}$
π_{Brent}	0.3480	-0.0335	-0.0884	0.0708	0.1286
π_{gas}	0.2185	0.1471	-0.0304	-0.0925	0.1230
$\%\Delta\pi$	0.1150	-0.1281	-0.0402	-0.0241	-0.0448
$\%\Delta Y_{d,US}$	-0.1762	-0.0799	0.0009	-0.5552	0.0608
$\%\Delta E_{\text{EUR-USD}}$	-0.0193	-0.1993	0.0048	0.0297	0.2983

Table 15: Point Estimates of Coefficient Matrix B (Model 2)

	$\%\Delta\pi$	$\%\Delta Y_{d,US}$	$\%\Delta E_{\text{EUR-USD}}$
$\%\Delta\pi$	-0.0307	-0.0303	-0.0573
$\%\Delta Y_{d,US}$	-0.0034	-0.5395	0.0441
$\%\Delta E_{\text{EUR-USD}}$	-0.0039	0.0357	0.2857

Table 16: Point Estimates of Coefficient Matrix B (Model 3)

	π_{Brent}	π_{gas}	$\%\Delta\pi$	$GECON$	$\%\Delta i$	$\%\Delta Y_{d,US}$	$\%\Delta E_{\text{EUR-USD}}$
π_{Brent}	0.4075	-0.0105	-0.1130	-0.1175	0.0960	0.0491	0.1452
π_{gas}	0.1205	0.1013	-0.0064	0.1877	-0.0625	-0.0528	0.1068
$\%\Delta\pi$	0.1097	-0.1528	-0.0246	0.0234	-0.0693	-0.0186	-0.0578
$GECON$	0.3950	0.0446	0.0161	0.3285	-0.0848	0.1525	0.0224
$\%\Delta i$	0.0276	0.1954	0.1279	-0.0782	0.2055	-0.0683	-0.0884
$\%\Delta Y_{d,US}$	0.0368	0.0052	-0.0052	-0.4184	0.0042	-0.6271	0.0971
$\%\Delta E_{\text{EUR-USD}}$	-0.1053	-0.2824	0.0775	0.1776	-0.2703	0.0605	0.2637

F Bayesian D matrices Model 2-3

Table 17: Point Estimates for structural matrix D (mean of posterior) — Model 2

	$\%\Delta\pi$	$\%\Delta Y_{d,US}$	$\%\Delta E_{\text{EUR-USD}}$
$\%\Delta\pi$	0.1076	0.9371	0.4075
$\%\Delta Y_{d,US}$	-1.1290	-0.0069	-0.6174
$\%\Delta E_{\text{EUR-USD}}$	-0.7515	-0.6992	0.3398

Table 18: Point Estimates for structural matrix D (mean of posterior) — Model 3

	π_{Brent}	π_{gas}	$\%\Delta\pi$	$GECON$	$\%\Delta i$	$\%\Delta Y_{d,US}$	$\%\Delta E_{\text{EUR-USD}}$
π_{Brent}	-0.5291	0.0584	-0.1576	0.3913	0.1422	-0.0497	-0.0072
π_{gas}	0.0293	-0.3648	-0.2943	0.0149	0.0391	0.0054	-0.0456
$\Delta\pi$	0.4345	0.4412	0.1870	0.4162	0.4681	0.4265	0.3851
$GECON$	0.3764	0.0431	-0.0828	-0.7399	-0.0355	0.0609	-0.0701
$\%\Delta i$	-0.1097	-0.1972	-0.4252	-0.2853	-0.4299	-0.2038	-0.2785
$\%\Delta Y_{d,US}$	0.0321	0.0340	-0.2548	-0.0349	0.0982	-0.5493	0.0307
$\%\Delta E_{\text{EUR-USD}}$	-0.1621	-0.1884	-0.0652	-0.1205	-0.1755	-0.2445	0.2902

G IRFs to structural shocks Bayesian Model 2-3

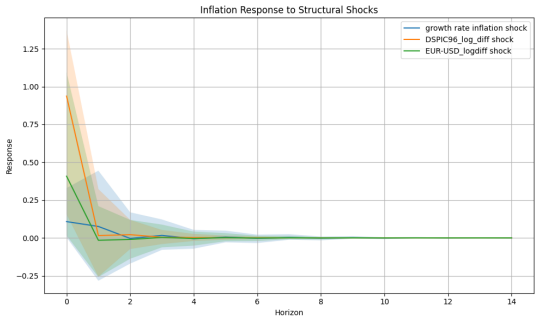

Figure 15: Impulse responses of Scenario 2 using non-recursive ordering

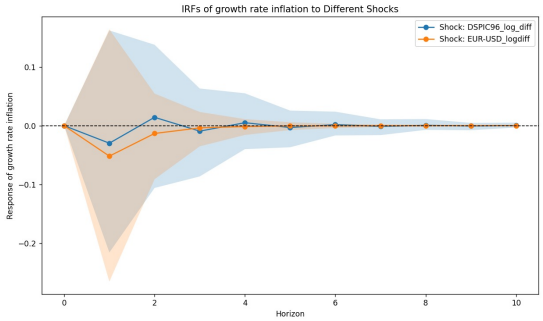

Figure 16: Impulse responses of Scenario 2 using recursive ordering

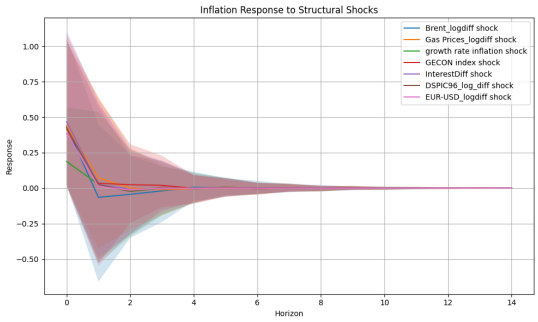

Figure 17: Impulse responses of Scenario 3 using non-recursive ordering

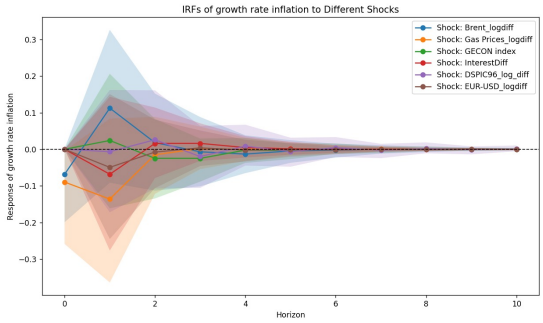

Figure 18: Impulse responses of Scenario 3 using recursive ordering

References

Agrippino, S. M. and Ricco, G. (2018). Bayesian vector autoregressions.

Andriantomanga, Z., Bolhuis, M. A., and Hakobyan, S. (2023). *Global supply chain disruptions: Challenges for inflation and monetary policy in Sub-Saharan Africa*. International Monetary Fund.

Asab, N. A. (2025). Are supply shocks a key driver of global inflation? evidence from cpi and gdp deflator analysis. *Research in Globalization*, 100279. Under a Creative Commons license.

Baumeister, C., Korobilis, D., and Lee, T. K. (2022). Energy markets and global economic conditions. *Review of Economics and Statistics*, 104(4):828–844.

Baumeister, C. and Peersman, G. (2013). Time-varying effects of oil supply shocks on the us economy. *American Economic Journal: Macroeconomics*, 5(4):1–28.

Bańbura, M., Bobeica, E., and Hernández, C. M. (2023). What drives core inflation? the role of supply shocks. *ECB Working Paper Series*, (2875).

Bennett, H. (2024). Measuring inflation: Headline, core and supercore services. Federal Reserve Bank of St. Louis, On the Economy Blog.

Bernanke, B. S., Boivin, J., and Eliasz, P. (2005). Measuring the effects of monetary policy: A factor-augmented vector autoregressive (favar) approach. *The Quarterly Journal of Economics*, 120(1):387–422.

Blanchard, O. J. and Quah, D. (1988). The dynamic effects of aggregate demand and supply disturbances. Technical report, Economic Department, MIT. Working Paper.

Chan, J. C. (2021). Minnesota-type adaptive hierarchical priors for large bayesian vars. *International Journal of Forecasting*, 37(3):1212–1226.

Clarida, R., Gali, J., and Gertler, M. (1999). The science of monetary policy: A new keynesian perspective. *Journal of Economic Literature*, 37(4):1661–1707.

Coulombe, P. G., Leroux, M., Stevanovic, D., and Surprenant, S. (2020). How is machine learning useful for macroeconomic forecasting? *arXiv preprint arXiv:2008.12477*.

Di Giovanni, J., Kalemli-Özcan, Silva, A., and Yildirim, M. A. (2022). Global supply chain pressures, international trade, and inflation.

Dungey, M. and Pagan, A. (2000). A structural var model of the australian economy. *Economic record*, 76(235):321–342.

Dynan, K. E., Skinner, J., and Zeldes, S. P. (2004). Do the rich save more? *Journal of political economy*, 112(2):397–444.

Eickmeier, S., Metiu, N., and Prieto, E. (2023). Global supply chain shocks and euro area inflation. VoxEU Column or Working Paper. Adjust once you confirm the exact citation (VoxEU or official WP).

Ferrante, F. et al. (2023). Inflation in the time of covid: The role of supply bottlenecks. *FEDS Notes*.

Finck, D. and Tillmann, P. (2022). Global supply chain shocks and euro area inflation. CESifo Working Paper. Add official working paper number if available.

Giannone, D., Lenza, M., and Primiceri, G. E. (2015). Prior selection for vector autoregressions. *Review of Economics and Statistics*, 97(2):436–451.

Goldberg, P. K. and Knetter, M. M. (1997). Causes and consequences of the export enhancement program for wheat. In *The effects of US trade protection and promotion policies*, pages 273–296. University of Chicago Press.

Hofmann, B., Manea, C., and Mojon, B. (2024). Targeted taylor rules: Monetary policy responses to demand- and supply-driven inflation. *BIS Quarterly Review*, 2024(December):19–31.

Kilian, L. and Lütkepohl, H. (2017). *Structural Vector Autoregressive Analysis*. Cambridge University Press, Cambridge.

Kilian, L. and Murphy, D. P. (2012). Why agnostic sign restrictions are not enough: Understanding the dynamics of oil market var models. *Journal of the European Economic Association*, 10(5):1166–1188.

Kilian, L. and Murphy, D. P. (2014). The role of inventories and speculative trading in the global market for crude oil. *Journal of Applied econometrics*, 29(3):454–478.

Lewandowski, D., Kurowicka, D., and Joe, H. (2009). Generating random correlation matrices based on vines and extended onion method. *Journal of Multivariate Analysis*, 100(9):1989–2001.

Litterman, R. B. (1986). Forecasting with Bayesian Vector Autoregressions-Five Years of Experience. *Journal of Business & Economic Statistics*, 4(1):25–38.

McCracken, M. W. and Ngân, T. K. (2023). Using core inflation to predict headline inflation. Federal Reserve Bank of St. Louis, On the Economy Blog.

Nair, S. and Deepa, N. (2023). Forecasting cost-push inflation with lasso over ridge regression. pages 64–70.

Obstfeld, M. and Rogoff, K. (2000). The six major puzzles in international macroeconomics: Is there a common cause? *NBER Macroeconomics Annual*, 15. Free access.

Shapiro, A. H. (2022). Supply-driven inflation: Evidence from the u.s. *FRBSF Economic Letter*.

Sims, C. A. (1980). Macroeconomics and reality. *Econometrica: journal of the Econometric Society*, pages 1–48.

Wang, S. L. and McPhail, L. (2014). Impacts of energy shocks on us agricultural productivity growth and commodity prices—a structural var analysis. *Energy Economics*, 46:435–444.